An evaluation study of miniature dielectric crossed compound parabolic concentrator (dCCPC) panel as skylights in building energy simulation

Meng Tian [a], Li Zhang [a], Yuehong Su [a,*], Qingdong Xuan [b], Guiqiang Li [b, c,*], Hui Lv [d]

[a] Department of Architecture and Built Environment, Faculty of Engineering, University of Nottingham, University Park, Nottingham, NG7 2RD, UK

[b] Department of Thermal Science and Energy Engineering, University of Science and Technology of China, 96 Jinzhai Road, Hefei, 230026, China

[c] School of Engineering, University of Hull, Hull, HU6 7RX, UK

[d] Hubei Collaborative Innovation Center for High-efficiency Utilization of Solar Energy, Hubei University of Technology, Wuhan, 430068, China

* Corresponding authors: yuehong.su@nottingham.ac.uk, Guiqiang.Li@hull.ac.uk

Abstract

The potential of miniature dielectric crossed compound parabolic concentrator (dCCPC) panel as skylights for daylighting control has drawn a considerable research attention in the recent years, owing to its feature of variable transmittance according to the sun position, but the viability of using it as skylights in buildings has not been explored yet comprehensively. This paper aims to study the feasibility of utilizing miniature dCCPC panel as skylight in different locations under various climates in terms of energy saving potential besides its daylighting control function. The transmittance of dCCPC panel varies at every moment according to the sky condition and sun position. Due to this specific property, this study novelly implemented a polynomial formula of the dCCPC transmittance in the Grasshopper platform, from which EnergyPlus weather data can be called to calculate the hourly transmittance data of dCCPC skylight panel throughout the whole year. An hourly schedule of transmittance is generated according to the hourly sky condition determined by the daylight simulation through Radiance and Daysim, and is then input to EnergyPlus simulation to predict the energy consumption of a building with dCCPC skylight. Fourteen locations around the world are therefore compared to find the most appropriate place for using miniature dCCPC panel as skylights. The energy saving in cooling, heating and lighting with use of dCCPC skylight panel are investigated and compared with low-E and normal double glazing. The results show that the dCCPC skylight panel can reduce cooling load by mitigating solar heat gain effectively although its performance is affected by several criteria such as sky conditions and local climates. It is generally more suitable for the locations with longer hot seasons, e.g., Log Angeles, Miami, Bangkok and Manila, in which dCCPC could provide up to 13% reduction in annual energy consumption of building. For the locations having temperate and continental climates like Beijing, Rome, Istanbul and Hong Kong, a small annual energy saving from 1% to 5% could be obtained by using dCCPC skylight panel.

Keywords

Dielectric crossed compound parabolic concentrator (dCCPC); daylighting control; Grasshopper; energy saving.

Nomenclature

Abbreviations

DB	Double glazing
dCCPC	Dielectric crossed compound parabolic concentrator
dCCPC-lowE	Low-E double glazing with dCCPC inside
dCCPC-DB	Double glazing with dCCPC inside
SHGC	Solar heat gain coefficient
VT	Visible transmittance

General symbols

I	Direct normal solar irradiance ($\mathrm{W/m^2}$)
I_{total}	Total irradiance ($\mathrm{W/m^2}$)
I'	Equivalent direct normal solar irradiance for a tilted surface ($\mathrm{W/m^2}$)
$I_h{}'$	Equivalent diffuse horizontal irradiance for a tilted surface ($\mathrm{W/m^2}$)
T_0	Transmittance of dCCPC under overcast sky
T_{dCCPC}	Transmittance of dCCPC
Z	Solar zenith angle (°)
Z'	Equivalent solar zenith angle for a tilted surface (°)
a_n, b_n, c_n	Regression coefficients
k	Constant coefficient
β	Tilt angle of dCCPC entry aperture (°)
γ	Solar azimuth angle (°)
γ'	Equivalent solar azimuth angle for a tilted surface (°)
$\Delta\gamma'$	Relative equivalent azimuth angle for a tilted surface (°)
ε	Sky clearness factor
ε'	Equivalent sky clearness factor for a tilted surface
θ_i	Incident angle on the entry aperture of dCCPC (°)
θ_h	Solar altitude angle (°)
θ_h'	Equivalent solar altitude angle for a tilted surface (°)

1. Introduction

The energy consumption in buildings takes more than one-third of total global energy consumption (Lowry, 2016). The electricity required by artificial lighting is one of the main parts of the energy demand for buildings. In the solar heating & cooling (SHC) programme in 2015 held by the international energy agency, it was stated that the lighting energy took 19% (2900 TWh) of the total global electricity consumption approximately, and it is estimated to reach 4250 TWh by 2030 under current policies (Attia et al., 2017, SHC, 2015). Daylighting design is a popular choice in modern building design with the considerations of energy saving, visual comfort and hence occupant health. The combination of direct sunlight and diffuse skylight are regarded as daylight whose quality and intensity varies depending on the location, season, time, weather, sky condition and so forth. With an appropriate daylighting design, about 40% lighting energy could be saved (Dubois and Blomsterberg, 2011), and this could even reach 70% with the proper designs of space type and control type (Ahadi et al., 2017). As a passive solar energy application, daylighting is accompanied with solar heating which can reduce the heating load in winter to some extent. It was also found by many researchers that daylight is good for human health by curing medical ailments and reducing psychological sadness related to the seasonal affective disorder (Hraska, 2015, Wong, 2017, Liberman, 1990). In a survey conducted by Hourani et al. (Hourani and Hammad, 2012), more than 80% of the working staffs were willing to sit by windows and similar results were obtained from the student and patient groups. Daylight also results in the better perception and higher productivity for occupants (Sivaji et al., 2013, S. R. Kellert et al., 2008).

As one type of the nonimaging optics, compound parabolic concentrator has been attempted to be utilized in building facade for daylighting application in the past decades. Walze et al. (Walze et al., 2005) proposed two kinds of smart windows with the microstructure of two dimensional (2D) compound parabolic concentrator (CPC) array on the surface, which focused on preventing unnecessary solar radiation and improving light-guiding abilities. Yu et al. (Yu et al., 2014) investigated the feasibility of 2D dielectric CPC in daylighting control as it is used as a skylight and found that the transmittance of the stationary CPC varies with the sun positions, which is lower at noon and larger in the morning and afternoon. Li et al. proposed a lens-walled CPC panel integrating photovoltaic and daylighting control that can generate electricity and decrease the indoor illuminance level (Li et al., 2018, Li, 2018). Ulavi et al. (Ulavi et al., 2014b, Ulavi et al., 2014a) designed a hybrid solar window integrating tubular absorber and 2D CPC for the purpose of transmitting daylight to the interior and concentrate solar radiation onto the absorber at the same time. Another hybrid window called PRIDE also works in the similar way but replacing the tubular absorber with photovoltaic (PVEducation) module to generate electricity. With the improvements by many researchers (Zacharopoulos et al., 2000, Mallick et al., 2004, Mallick et al., 2006, Mallick and Eames, 2007, Sarmah and Mallick, 2015, Sarmah et al., 2014, Baig et al., 2014), the electricity generated by the latest generation of PRIDE is 3.17 times higher than that from a flat PV of same size and it also provides daylighting to the interior simultaneously.

Although the visual environment provided by daylight is preferred by occupants, the glare that is the result of extreme contrast within the vision field caused by direct sunlight is a key point that should be considered in daylighting design. Various diffuse panel becomes more popular in skylight due to creating better visual environment and saving lighting energy with the advantages of redirecting direct sunlight. Many companies has produced and sold various diffuse skylight panels for real building application. For example, the prismatic diffuse panel designed by Excelite (Excelite, n.d.), the highly diffused Quasar prismatic skylight produced by Kingspan (Kingspan, n.d.), the different prismatic skylights provided by AcuityBrands (AcuityBrands, n.d.), and etc. From our previous research (Tian and Su, 2015, Tian and Su, 2016), it is found that a dielectric crossed CPC (dCCPC) panel as skylight also has an outstanding performance in preventing glare by reflecting back direct sunlight when it is strong around the midday. Further to such daylight control feature, the effect of dCCPC skylight panel on the energy performance of a building will be investigated in this paper to evaluate its implication and suitability in actual applications.

As is known, the transmittance of a dCCPC panel varies with sky condition and sun position, which means that it would not be a constant value for different time points. A polynomial formula for their relationship has been obtained in our previous study (Tian and Su, 2018a). In this paper, a novel method implementing this polynomial model in Grasshopper is proposed in order to investigate the energy performance of a building with dCCPC skylight panel. The continuously changed transmittance of dCCPC can be calculated in Grasshopper and fed to the dynamic simulation of building energy consumption in EnergyPlus. Fourteen locations are selected around the world for the simulation, in which the dCCPC panel will be compared with traditional double glazing and low-E double glazing. The main criteria used in evaluation are the effects of dCCPC on thermal load, lighting energy consumption and total energy consumption in buildings. The advantages and drawbacks of dCCPC skylight panel are discussed, and the feasibilities of practical application are summarized in terms of overall energy saving at the end of this research.

2. Methodology

2.1. Introduction of software for energy simulation

In this study, the building energy simulation package, EnergyPlus, and the lighting analysis tool, Radiance/Daysim will be used to determine the hourly energy and daylighting performance of an example building with dCCPC skylight panels. However, the time-varying feature of the transmittance of dCCPC panel needs to be dealt with tactically using Grasshopper within the Rhinoceros 3D. A multiple nonlinear regression (MNLR) model proposed by Tian and Su (Tian and Su, 2018a) which determines the transmittance of dCCPC according to the sun position and sky condition, is applied and modified in order to calculate the transmittance of dCCPC in arbitrary tilt angles under various sky conditions. The details of calculating the hourly transmittance data of dCCPC panel by MNLR model is introduced in Section 3. The point to incorporate the dCCPC transmittance model in simulations is illustrated in the workflow diagram in Fig. 1. In the platform grasshopper in Rhinoceros 3D, the transmittance schedule of dCCPC is generated hourly by programming MNLR model in grasshopper, and then the required criteria sun position and sky condition are calculated by the imported EnergyPlus weather data and daylight simulation run by Radiance and Daysim. The annual lighting schedule can be then obtained by daylighting simulation through

Radiance/Daysim according to the transmittance schedule of dCCPC. Finally, the energy consumption of building is simulated by the energy analysis through EnergyPlus.

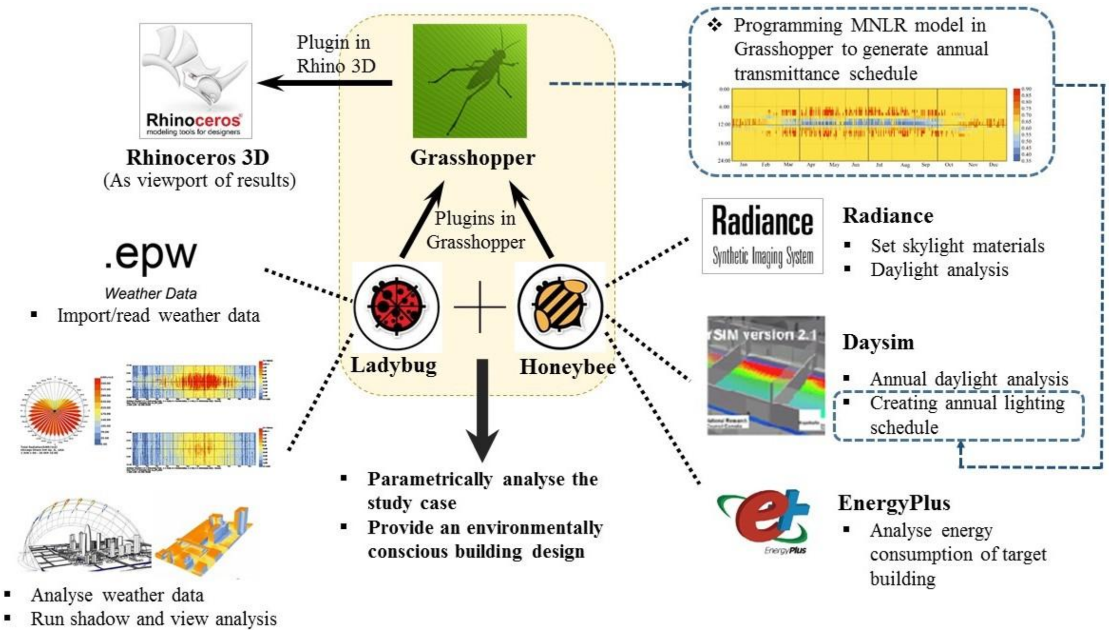

Fig. 1. Workflow diagram of running daylighting and energy simulation for the building model in Grasshopper

Rhinoceros 3D is a three-dimensional (3D) computer graphics and computer-aided design application software that is good at modelling curves and freeform surfaces in computer graphics (Rhinoceros, n.d.). Grasshopper is one of the key plugins running within the Rhinoceros 3D, which is a visual programming language and environment to build generative algorithms (Grasshopper, n.d.). Programs can be created by dragging provided components onto a canvas and connecting each component. Ladybug and Honeybee are two plugins for Grasshopper to import and analyse standard weather data, and run simulations for building energy, occupant comfort, daylighting usage and lighting energy consumption with the simulation engines like EnergyPlus, Radiance, Daysim and OpenStudio, etc. Radiance is a widely used optical simulation tool for analysing the distribution of visible radiation in illuminated spaces based on the backward ray-tracing from the image plane to the sources (Radiance, 2014). Daysim is a Radiance-based simulation engine in Rhinoceros for predicting the annual daylighting performance in building, analysing complex shading and lighting control system (Jakubiec and Reinhart, 2012). EnergyPlus and OpenStudio are the console-based software which is good at simulating the energy consumption including heating, cooling, ventilation, lighting and water usage in buildings (EnergyPlus, 2017). Therefore, a building can be modelled and analysed in Grasshopper parametrically for both comprehensive design and accurate energy evaluation.

2.2. Building model description

The model of an example building is set as a single-storey office building with skylights and windows as shown in Fig. 2, in which the sun path diagram of Birmingham, UK (52.45°N, 1.73°W) is illustrated with the yellow circles indicating the sun positions from 4am to 8pm on 21st June. The building is assumed to have the dimension of 80m (L) × 30m (W) × 3m (H) referring to the typical size of standard air-conditioned office building (CIBSE, 2000), and the longitudinal sides of the building are in east-west direction. The window-to-wall ratio (WWR) is set to be 0.35 for the walls in south, north, east and west directions, which is within the optimal range of WWR for most office buildings in different climates (Goia et al., 2013, Goia, 2016). The total area of skylights follows the general rule of thumb, i.e., 5% of roof area. The total number of skylights are 84 and located on the roof regularly in a 14×6 array. The skylights are mounted on the flat roof and tilted to the south. The tilt angle of dCCPC stays unchanged for the whole year but is different for each city. The tilt angle and the solar altitude angle at 12:30pm on 21st June in each location are complementary to achieve the best performance.

The interior of the office building is open plan. The reflectance values of internal surfaces are 0.2 for the floor, 0.5 for the walls and 0.8 for the ceiling according to the typical reflectance values of room surfaces (LightingResearchCenter, n.d.). The work plane whose illuminance distribution would be simulated is taken as 0.8m above floor level. In the following energy simulations in Grasshopper, the 'OpenOffice' schedules are used for occupancy, activities, heating, cooling, equipment and infiltration. The walls, windows, roof and floor are set as the default exterior wall, clear double glazing window, exterior roof and exterior floor constructions provided by EnergyPlus, respectively. The default constructions may not be the best selections for the purpose of energy saving for building, but can be considered as the constructions with average performances that are more suitable for analysing the effect of skylights in different climates. Similarly, the heating and cooling load in simulations are calculated by using the ideal loads air system template, which aims to focus on the variation of thermal load caused by skylights rather than different air-conditioning systems. The heating set point is 21°C and cooling set point is 24°C. It is important to mention that, the control types of artificial lighting for all models are the same, which is auto dimming and it will be switched off when there is no occupancy in the room. The sensor points of lighting and lighting control are located in a 13×5 array detecting the illuminance level of working plane. The set point of lighting is 500lux. Shading and glare control are not considered for windows and skylights.

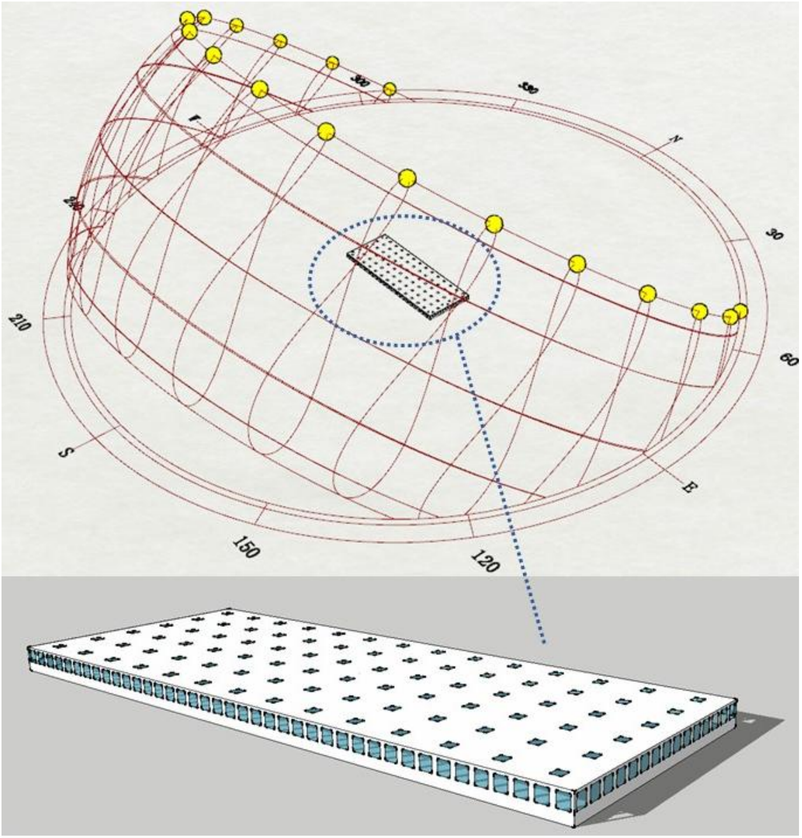

Fig. 2. Building model and sun path on 21st June from 4am to 8pm in Birmingham

2.3. Skylights model description

In order to investigate the effect of dCCPC panel on building energy performance, three types of skylight panels as listed in Table 1 will be compared. The basic skylight type as a reference is a typical clear double glazing window (DB) with a visible transmittance (VT) of 0.79, solar heat gain coefficient (SHGC) of 0.70 and U-value of 2.669 W/m^{2}K (EWC, n.d.).The other two types of skylight panels are with a dCCPC panel sandwiched within a clear double glazing (dCCPC-DB) and a low-E double glazing (dCCPC-lowE), respectively, as shown in Fig. 3. Thus the dCCPC-DB and dCCPC-lowE skylight panels are still in the form of double glazing and can be assumed to have the same U-value as the original double glazing. The U-value, VT and SHGC for typical low-E double glazing is 1.420 W/m^{2}K, 0.69 and 0.27 respectively (EWC, n.d.). To give VT and SHGC values of the dCCPC-DB and dCCPC-lowE skylight panels, the original values of double glazing may be multiplied by the transmittance of dCCPC panel, calculation of which is explained in Section 3 in details.

Table 1. Properties of skylight panels (DB, dCCPC-DB and dCCPC-lowE)

	Clear double glazing (DB)	Clear double glazing with dCCPC (dCCPC-DB)	Low-E double glazing with dCCPC (dCCPC-lowE)
U-value (W/m^{2}K)	2.669	2.669	1.420
SHGC	0.70	$T_{dCCPC} \times 0.70$	$T_{dCCPC} \times 0.27$
VT	0.79	$T_{dCCPC} \times 0.79$	$T_{dCCPC} \times 0.69$
T_{dCCPC}: Transmittance of dCCPC			

The detailed dimensions of the dCCPC panel used in simulations is demonstrated in Fig. 3 below. The dimension of the entry aperture for each element in the panel is 0.018m × 0.018m. A top cover with the thickness of 1mm is used to connect the individual element into a panel. Both of the width and length of the dCCPC panel are about 1.42m so that each panel consists of 66×66 individual components. The thickness of dCCPC panel is 24.3mm. The inner and outer half acceptance angle of dCCPC are 14.47° and 22.02°. The material of dCCPC is acrylic with the refractive index of 1.49.

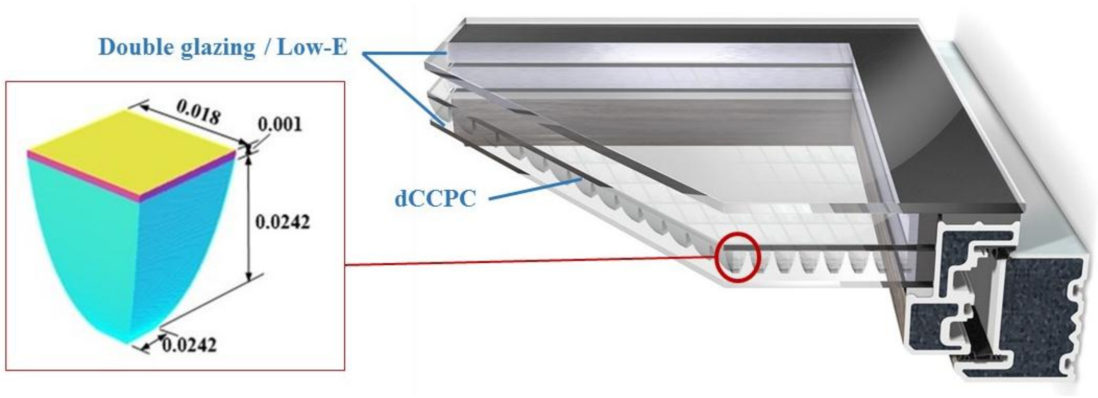

Fig. 3. Dimension of dCCPC panel

2.4. Location

In order to investigate the performance of dCCPC skylight panel in different locations and climates, 14 cities are chosen for energy simulation of the example office building. The 14 cities in Table 2 includes the locations from the eastern hemisphere to western hemisphere on earth. Two of them are in America, six of them are in Europe and the rest six are in Asia. According to the Köppen-Geiger climate classification, the climates of the fourteen cities cover four main categories which are tropical climate, dry climate, temperate climate and continental climate. Among all cities, some locations need either only cooling or heating such as Bangkok and Kiruna, and others require both during the whole year like Beijing and Istanbul. Some cities have strong direct sunlight like Lhasa, and some cities are covered by clouds in most of the time like Aberdeen. The sky condition is one of the key factors determining the transmittance of dCCPC panel, the percentage coverage by different sky conditions during the daytime of whole year for each location are demonstrated in Fig. 4. The sky conditions are calculated according to the annual weather data and categorized by sky clearness factor proposed by Perez, et al. (Perez et al., 1990). Because the performance of dCCPC is determined by sky conditions, it is important to point out that the sky conditions are calculated for the daytime simulations, while the sky conditions are assumed as overcast sky in the night, that is, the transmittance of dCCPC under overcast sky is used as the transmittance of dCCPC for night time in simulation. It can be found that the percentages of clear sky are around or less than 10% for most cities, except for Lhasa, Los Angeles and Miami. Aberdeen has the longest time of overcast sky. The overcast and overcast to intermediate sky take about 90% time of the whole year.

Table 2. Locations and climates of simulated cities

Location		Latitude	Longitude	Köppen-Geiger climate classification	
Asia	China-Beijing	39.80°	116.47°	Dwa	Continental dry winter and hot summer climate
	China-Hong Kong	22.32°	114.17°	Cfa	Hot summer temperate without dry season climate
	China-Shanghai	31.17°	121.43°	Cfa	Hot summer temperate without dry season climate
	China-Lhasa	29.67°	91.13°	BSK	Arid steppe cold climate
	Philippines-Manila	14.52°	121.00°	Aw	Tropical savanna wet climate
	Thailand-Bangkok	13.92°	100.60°	Aw	Tropical savanna wet climate
Europe	Finland-Helsinki	60.32°	24.97°	Dfb	Warm summer continental without dry season climate
	UK-Aberdeen	57.20°	-2.22°	BSK	Arid steppe cold climate
	UK-Birmingham	52.45°	-1.73°	Cfb	Warm summer temperate without dry season climate
	Italy-Rome	41.80°	12.58°	Csa	Temperate dry and hot summer climate
	Sweden-Kiruna	67.82°	20.33°	Dfc	Hot summer continental without dry season climate
	Turkey-Istanbul	40.97°	28.82°	Csa	Temperate dry and hot summer climate
America	USA-Los Angeles	33.93°	-118.40°	Csa	Temperate dry and hot summer climate
	USA-Miami	25.80°	-80.27°	Aw	Tropical savanna wet climate

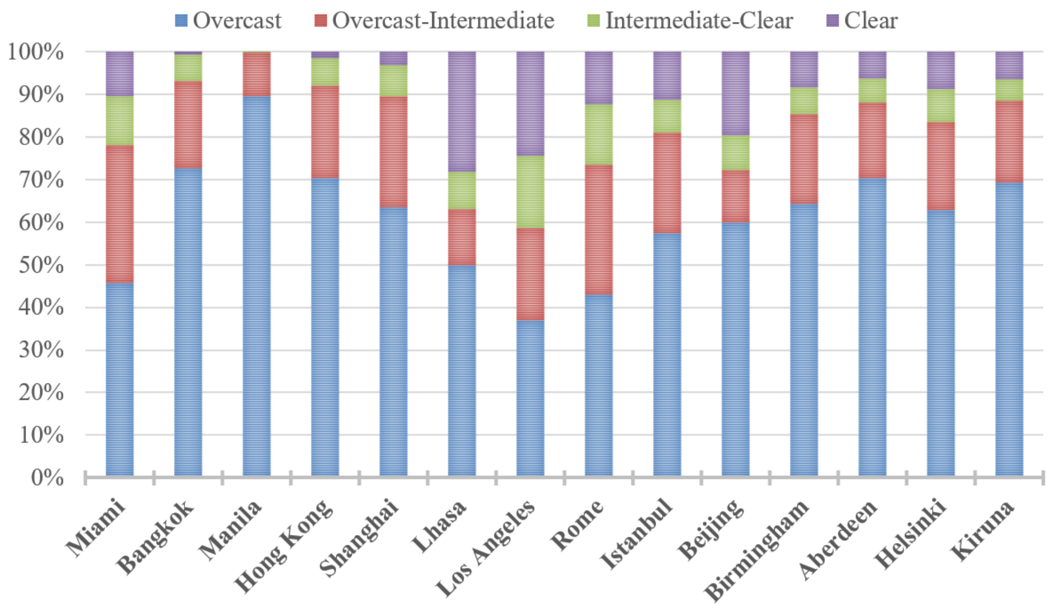

Fig. 4. Percentage of daytime for different sky conditions during a whole year for selected locations

3. Calculation of the transmittance of a tilted dCCPC from equivalent altitude and azimuth angles and equivalent sky clearness factor

The transmittance of dCCPC varies at every moment according to the sun position and sky condition, particularly exhibiting a feature of acceptance angle, which is favourable for daylighting control (Tian et al., 2017, Tian and Su, 2016, Tian and Su, 2018b). In order to simulate the energy performance of building using dCCPC as skylight, calculating the variable transmittance of dCCPC accurately for every simulation time step becomes the key to finish the whole simulation of this study.

In our previous study (Tian and Su, 2018a), a multiple nonlinear regression model, as shown in Eq. (1), has been proposed to correlate the transmittance of a horizontal dCCPC with the altitude and azimuth angles and sky clearness factor, and the coefficient of determination (R^2) is up to 0.944. However, when a dCCPC panel is used as skylights, its tilt angle should be adjusted according to the local latitude to maximise solar utilization. In order to fit this regression model, the equivalent altitude and azimuth angles and equivalent sky clearness factor with reference to a tilted surface are proposed and applied to calculate the transmittance of dCCPC used in the building energy simulation under given sky conditions in this study, as expressed in Eq. (2). This section introduces how to calculate those and an example of the whole process of calculating the transmittance of dCCPC in a specific moment is given.

$$T_{dCCPC} = \begin{cases} a_1 \cos(b_1\theta_h + b_2)\cos(b_3\gamma + b_4)\,(c_1 + c_2\varepsilon + c_3\gamma + c_4\theta_h \\ +c_5\theta_h\gamma + c_6\varepsilon\gamma + c_7\theta_h\varepsilon + c_8\varepsilon^2\theta_h\gamma + c_9\theta_h^2\varepsilon\gamma + c_{10}\gamma^2\varepsilon\theta_h, & \varepsilon > 1.2 \\ +c_{11}\varepsilon^2\theta_h^2\gamma^2 + c_{12}\varepsilon^2 + c_{13}\theta_h^2 + c_{14}\gamma^2) + a_2 & \\ T_0, & 1 \le \varepsilon \le 1.2 \end{cases} \tag{1}$$

Where θ_h is altitude; γ is azimuth; ε is sky clearness factor; T_{dCCPC} is the transmittance of dCCPC; a_n, b_n, c_n are regression coefficients; T_0 is the transmittance of dCCPC under overcast sky.

$$T_{dCCPC} = \begin{cases} \begin{array}{c} a_1 \cos(b_1\theta_h{}' + b_2) \cos(b_3\Delta\gamma' + b_4)\,(c_1 + c_2\varepsilon' + c_3\Delta\gamma' + c_4\theta_h{}' \\ +c_5\theta_h'\Delta\gamma' + c_6\varepsilon'\Delta\gamma' + c_7\theta_h'\varepsilon' + c_8\varepsilon'^2\theta_h'\Delta\gamma' + c_9\theta_h'^2\varepsilon'\Delta\gamma' \\ +c_{10}\Delta\gamma'^2\varepsilon'\theta_h{}' + c_{11}\varepsilon'^2\theta_h'^2\Delta\gamma'^2 + c_{12}\varepsilon'^2 + c_{13}\theta_h'^2 + c_{14}\Delta\gamma'^2) + a_2 \end{array} & ,\varepsilon > 1.2 \\ T_0, & 1 \le \varepsilon \le 1.2 \end{cases} \tag{2}$$

Where θ_h' is equivalent altitude (expressed in radian measure), $0^\circ < \theta_h' \le 90^\circ$; $\Delta\gamma'$ is relative equivalent azimuth (expressed in radian measure), $0^\circ \le \Delta\gamma' \le 45^\circ$, and $\Delta\gamma' = 0^\circ$ when the incident plane to the entry aperture of dCCPC is parallel to either side of its square entry aperture; ε' is equivalent sky clearness factor.

3.1. Description of coordinate system

For the purpose of calculating the equivalent altitude and azimuth angles of dCCPC, a coordinate system is applied as illustrated in Fig. 5. The south, east and zenith directions are represented by x, y and z axis respectively. The incident sunlight is denoted by vector $\overrightarrow{SO}$. The actual altitude and azimuth are indicated by θ_h and γ. To obtain the best result of controlling daylight by dCCPC, the dCCPC would be tilted to the south when it is applied in the northern hemisphere. The entry aperture (top surface) of dCCPC, which is also the interface between air and dielectric material, is denoted by the plane ABCD. The plane ABCD is south-tilted by β from the horizontal plane, which stands for the tilt angle β of dCCPC, and which is also the angle between the surface normal line NN' of the plane ABCD and the z axis. M is the point lying on the surface ABCD and the direction of $\overrightarrow{OM}$ refers to the equivalent north direction of the plane ABCD; the projection of $\overrightarrow{OM}$ on the horizontal plane coincides exactly with the x axis. The vector $\overrightarrow{SO}$ refers to the incident ray and the vector $\overrightarrow{OS_1}$ indicates the refracted ray. S' is the projection of point S onto the horizontal, and E is the projection of point S onto the plane ABCD. Thus, in terms of the sun position, γ is the actual azimuth and the angle between $\overrightarrow{OM}$ and $\overrightarrow{OE}$ ($\angle MOE$) is the equivalent azimuth γ' for the entry aperture of tilted dCCPC; the angle between $\overrightarrow{OS}$ and $\overrightarrow{OS'}$ is the actual solar altitude θ_h and the angle between $\overrightarrow{OS}$ and $\overrightarrow{OE}$ is the equivalent altitude θ_h'. The surface NSEN' is the plane of incidence, and the line OS_1 lies on this plane. The angle between the vector $\overrightarrow{OS}$ and the vector $\overrightarrow{ON}$ is the incident angle θ_i on the entry aperture of dCCPC.

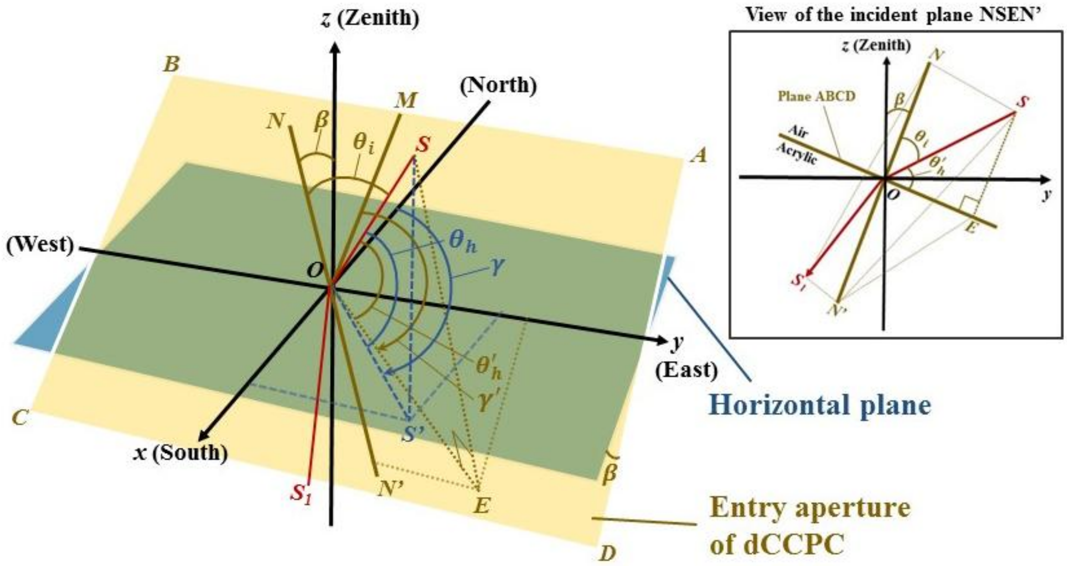

Fig. 5. Coordinate system of an optical path into a south-facing tilted dCCPC. S: sun position; $\overrightarrow{SO}$: incident ray; $\overrightarrow{OS_1}$: refracted ray; ABCD: entry aperture of tilted dCCPC; β: tilt angle; NN': surface normal of the plane ABCD; E: projection of point S onto the plane ABCD; S': projection of point S onto the horizontal plane; $\overrightarrow{OM}$: equivalent north direction of the plane ABCD; γ': equivalent solar azimuth angle.

3.2. Calculation of equivalent altitude angle

It is assumed that the lengths of the vector $\overrightarrow{OS}$ and $\overrightarrow{ON}$ are 1. The coordinates of point S and N can be expressed by:

$S(-\cos\theta_h \cos\gamma, \cos\theta_h \sin\gamma, \sin\theta_h)$ and $N(\sin\beta, 0, \cos\beta)$;

The vector $\overrightarrow{OS}$ and $\overrightarrow{ON}$ can be defined as:

$$\overrightarrow{OS} = (-\cos\theta_h \cos\gamma, \cos\theta_h \sin\gamma, \sin\theta_h) \quad (4)$$

and

$$\overrightarrow{ON} = (\sin\beta, 0, \cos\beta) \quad (5)$$

Then the angle between $\overrightarrow{OS}$ and $\overrightarrow{ON}$, that is, the incident angle θ_i, can be calculated by:

$$\cos\theta_i = \frac{\overrightarrow{OS} \cdot \overrightarrow{ON}}{|\overrightarrow{OS}| \cdot |\overrightarrow{ON}|} = -\cos\theta_h \cos\gamma \sin\beta + \sin\theta_h \cos\beta \quad (6)$$

Hence, the incident angle is

$$\theta_i = \mathrm{arc}(\cos\theta_i) \quad (7)$$

And the equivalent altitude of tilted dCCPC is:

$$\theta_h' = \frac{\pi}{2} - \theta_i \quad (8)$$

3.3. Calculation of equivalent azimuth angle

For the right triangle SOE with hypotenuse SO,

$$\left|\overrightarrow{ES}\right| = \left|\overrightarrow{OS}\right| \cdot \cos\theta_i = \cos\theta_i \qquad (9)$$

In addition, because $\overrightarrow{ON}$ and $\overrightarrow{ES}$ are two parallel vectors, the vector of $\overrightarrow{ES}$ can be expressed as:

$$\overrightarrow{ES} = (\cos\theta_i \sin\beta\,, 0, \cos\theta_i \cos\beta) \qquad (10)$$

The vector $\overrightarrow{EO}$ can be calculated by:

$$\overrightarrow{EO} = \overrightarrow{ES} + \overrightarrow{SO} \qquad (11)$$

Where $\overrightarrow{SO} = (\cos\theta_h \cos\gamma\,, -\cos\theta_h \sin\gamma\,, -\sin\theta_h)$ (12)

Thus,

$$\overrightarrow{EO} = (\cos\theta_h \cos\gamma + \cos\theta_i \sin\beta\,, -\cos\theta_h \sin\gamma\,, \cos\theta_i \cos\beta - \sin\theta_h) \qquad (13)$$

The vector $\overrightarrow{OM}$ is the equivalent north direction on the plane ABCD and the length of it is assumed to be 1. The coordinates of point M is:

$$M(-\cos\beta\,, 0, \sin\beta)$$

The angle γ' is the equivalent azimuth angle on the plane ABCD, which is defined by

$$\cos\gamma' = \frac{\overrightarrow{EO} \cdot \overrightarrow{OM}}{\left|\overrightarrow{EO}\right| \cdot \left|\overrightarrow{OM}\right|} \qquad (14)$$

$$\cos\gamma' = \frac{-\cos\theta_h \cos\gamma \cos\beta - \sin\theta_h \sin\beta}{\sqrt{(\cos\theta_h \cos\gamma + \cos\theta_i \sin\beta)^2 + \cos^2\theta_h \sin^2\gamma + (\cos\theta_i \cos\beta - \sin\theta_h)^2}} \qquad (15)$$

Considering the symmetry of dCCPC, only the range of 0°- 45° for the relative equivalent azimuth angle $\Delta\gamma'$ with reference to the symmetry needs to be used in calculating the transmittance of dCCPC. The relative equivalent azimuth angle $\Delta\gamma'$ can be given from γ' with reference to either of two symmetry lines of dCCPC:

$$\Delta\gamma' = \begin{cases} \operatorname{arc}(\cos\gamma') & if \quad \operatorname{arc}(\cos\gamma') \le 45^{\circ} \\ 90^{\circ} - \operatorname{arc}(\cos\gamma') & if \quad 45^{\circ} < \operatorname{arc}(\cos\gamma') < 90^{\circ} \\ \operatorname{arc}(\cos\gamma') - 90^{\circ} & if \quad 90^{\circ} \le \operatorname{arc}(\cos\gamma') \le 135^{\circ} \\ 180^{\circ} - \operatorname{arc}(\cos\gamma') & if \quad 135^{\circ} < \operatorname{arc}(\cos\gamma') \le 180^{\circ} \end{cases} \qquad (16)$$

Similarly, Equation (16) can be repeated for the range of 180°- 360°.

3.4. Example of calculating transmittance of dCCPC for random location, time and sky condition

An example of calculating the transmittance of dCCPC will be presented in this section in details. The location of Birmingham, UK(52.45°N, 1.73°W) and the local time 11am on 21st Dec were selected as an example. According to the EnergyPlus weather data (EnergyPlus, n.d.), the solar altitude θ_h is 12.8°, solar azimuth γ is 164.7°, and the direct normal irradiance I is 294W/m^2. The total irradiance I_{total} on the entry aperture of tilted dCCPC is 273 W/m^2 which was obtained by the simulation in Daysim using the EnergyPlus weather data.

In order to have a more daylighting control in summer, the tilt angle β of dCCPC was determined to be 37.55 $^\circ$.

From Eq. (4)-(8), the equivalent altitude θ_h' is

$$\theta_h' = 90^\circ - \text{arc}[\cos(-\cos\theta_h \cos\gamma \sin\beta + \sin\theta_h \cos\beta)] = 48.48^\circ \quad (17)$$

From Eq. (4)-(16), the relative equivalent azimuth $\Delta\gamma'$ can be calculated as 22.86°.

In order to calculate the transmittance of dCCPC, the equivalent sky clearness factor ε' is also required. The sky clearness factor ε is proposed in the sky model by Perez et al. (Perez et al., 1990): When $1 \leq \varepsilon \leq 1.2$, it refers to overcast sky; $\varepsilon \approx 1.2\sim2$ represents overcast to intermediate sky; $\varepsilon \approx 2\sim3$ indicates intermediate to clear sky; when $\varepsilon > 3$, it implies clear sky. According to the equation of calculating the sky clearness factor, the equivalent sky clearness factor can be expressed as

$$\varepsilon' = \frac{\frac{(I_h{}' + I')}{I_h{}'} + kZ'^3}{1 + kZ'^3} \qquad (18)$$

where I' is equivalent direct normal solar irradiance; $I_h{}'$ is equivalent diffuse horizontal irradiance; k is a constant and equals 1.041 for Z' in radians; Z' is equivalent solar zenith angle in radians. The values of $'$, $I_h{}'$ and Z' could be obtained as shown in Table 3.

The equivalent sky clearness factor ε' is 3.98 according to Eq. (18). Therefore, the transmittance of dCCPC can be calculated by Eq. (2) and the value of transmittance is 0.72. In addition, the transmittance obtained by Photopia simulation is 0.75, which provides a good agreement with the calculated result. All of the values obtained in example calculation are summarized in Table 3 below.

Table 3. Summary of the calculation process and values of symbols used in Example

Term	Calculation formula	Value of example	Step No.
β	$90^\circ - Latitude$	37.55°	1
$\Delta\gamma'$	Eq. (4)-(16)	22.86°	2
θ_h'	Eq. (17)	48.48°	3
Z'	$90^\circ - \theta_h'$	41.52°	4
I'	$I\cos\theta_i$	$220.13\,\mathrm{W/m^2}$	4
$I_h{}'$	$I_{total} - I'$	$52.87\,\mathrm{W/m^2}$	4
ε'	Eq. (18)	3.98	5
T_{dCCPC} from calculation	Eq. (2)	0.72	6
T_{dCCPC} from simulation	N/A	0.75	N/A

An example of hourly transmittance for a whole year when the dCCPC is used in Birmingham, UK (52.45°N, 1.73°W) are shown in Fig. 6. It can be found that the transmittance is lower in the morning and afternoon and higher at noon from November to February, and the transmittance variations are reversed from March to Oct. This actually indicates the daylighting control function of dCCPC.

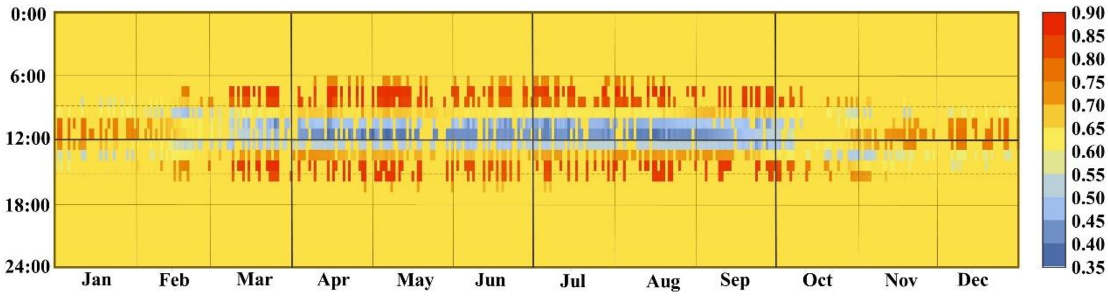

Fig. 6. Hourly transmittance of dCCPC for a whole year in Birmingham

4. Results of energy performance

4.1. An example of variations of hourly energy consumption

The particular characteristics of dCCPC panel is that its transmittance can vary with the sun position and sky condition. Before demonstrating the annual energy performance of building, a set of example results of Birmingham are provided to show the hourly variations of energy consumption, solar heat gain, skylight transmittance and sky conditions. In Fig. 7 and Fig. 8, it can be found how the transmittance of dCCPC-DB and dCCPC-lowE skylight panels varies with the sun position and sky clearness factor, and how they affect the solar heat gain and thermal load of building. The example city chosen is Birmingham, UK (52.45°N, 1.73°W), and the date is 22nd Jun which is a typical day in summer. Three kinds of skylights are compared, which are standard double glazing (DB), double glazing with a dCCPC layer (dCCPC–DB) and double glazing with low-E coating and a dCCPC layer (dCCPC–LowE).

Based on the sky clearness factor shown in Fig. 8, the sky is clear from 9am to 3pm, and the sky is intermediate or overcast in the morning and afternoon. In Fig. 7, the transmittance of DB stays almost constant about 0.8 and changes slightly as a result of Fresnel effect. The transmittance of dCCPC-DB and dCCPC-lowE varies as time goes on: the transmittance is higher in the morning and afternoon, and it becomes lower at noon. The total solar heat gain from skylight is affected by the transmittance significantly. For DB, the solar gain becomes higher from morning to noon, and then drops down in the afternoon. For dCCPC-DB, the solar gain also goes higher from morning to noon and decreases in the afternoon, but the solar gain is reduced at 11am, 12pm and 1pm due to the low transmittance at noon. For dCCPC-lowE, the total solar gain is less than 10kWh for all the time and has similar tendencies with dCCPC-DB. In terms of hourly solar gain, dCCPC-DB reduces more than half of the solar gain compared with DB. The solar gain by dCCPC-lowE is about a quarter of dCCPC-DB owing to the lower transmittance and SHGC. The solar gain also affects the total thermal load. In Birmingham on 22nd Jun, only cooling load is required. In Fig. 8, it is important to note that the thermal load here indicates cooling load because only cooling is required in this day. It can be seen that the demand of cooling starts from 11am and becomes high in the afternoon. Due to the less solar gain through dCCPC-DB and dCCPC-lowE, the cooling load of using these two skylights are less than that of using DB except 7pm. The reason is that at 19:00, outdoor illuminance becomes low and artificial lighting is required for dCCPC-DB and dCCPC-lowE. Lighting causes more thermal load so that the thermal load of DB is smaller at this time. For 12pm, 1pm and 2pm, when the solar gain from dCCPC-DB and dCCPC-lowE are much less than DB, more than 1/3 of cooling requirement are saved by dCCPC-DB and dCCPC-lowE compared to DB. The total cooling load savings of dCCPC-DB and dCCPC-lowE are 14.5% and 30% respectively for the whole day of 22nd Jun comparing with double glazing (DB).

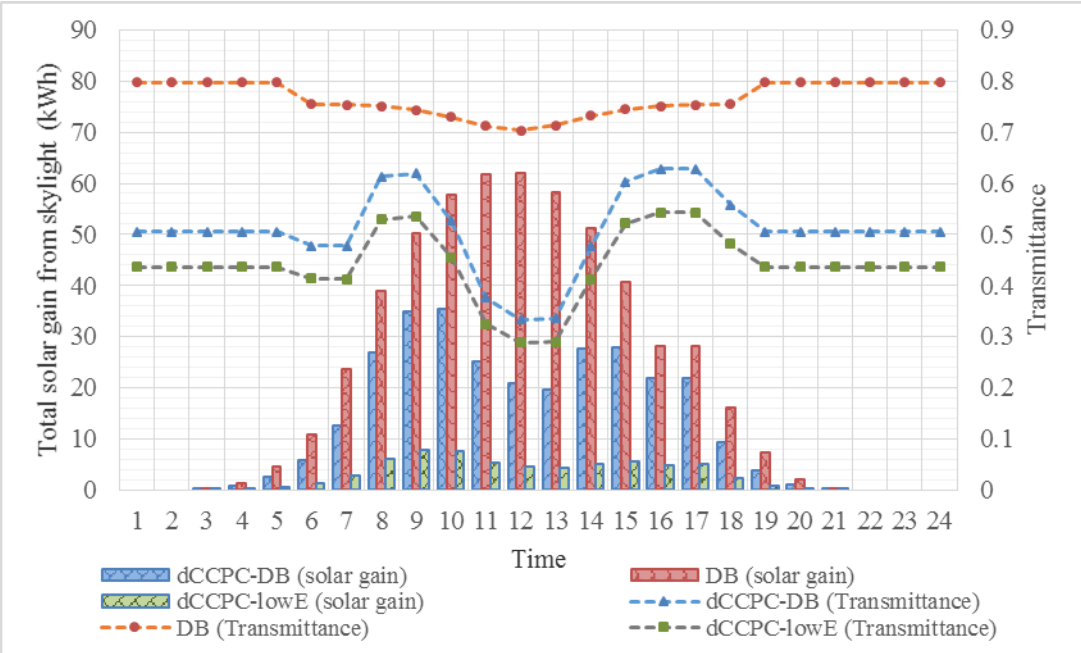

Fig. 7. Hourly sol from skylights and transmittance of skylights on 22nd Jun in Birmingham, UK (52.45°N, 1.73°W)

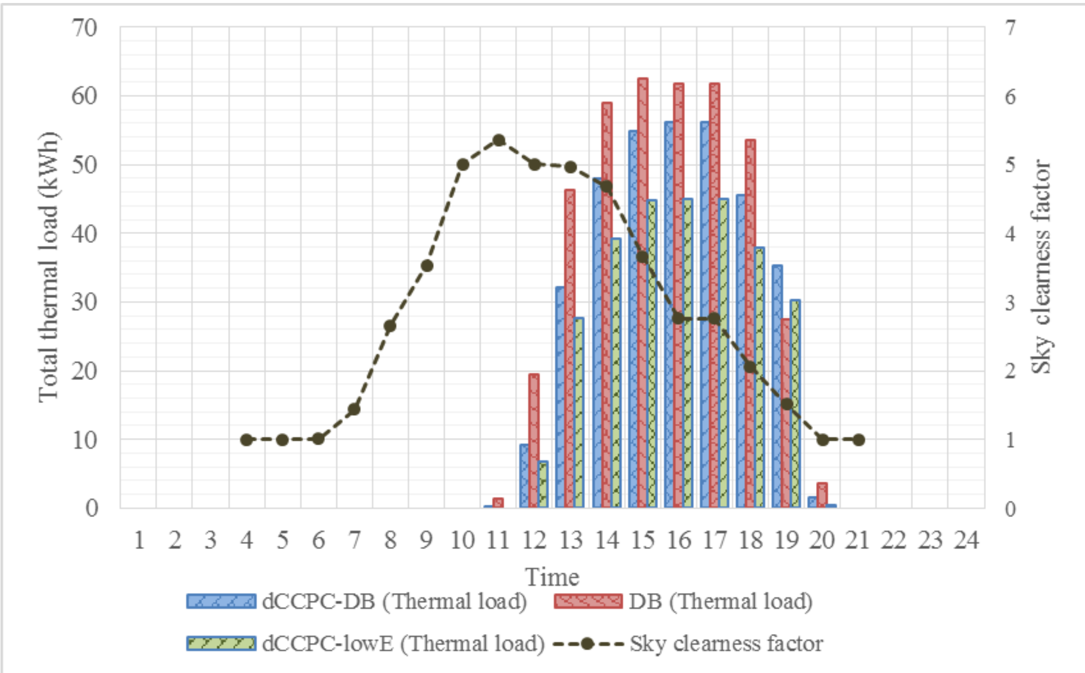

Fig. 8. Hourly total thermal load (cooling and/or heating) and sky clearness factor on 22nd Jun in Birmingham, UK (52.45°N, 1.73°W)

4.2. Monthly and annual thermal load

Based on the annual weather data and detailed model settings, the results of cooling and heating load of the example building are obtained and compared in this section. Fig. 9(a) and Fig. 9(b) illustrates the data of monthly cooling and heating loads when the building utilizes double glazing (DB), double glazing with dCCPC layer (dCCPC-DB) and low-E double glazing with dCCPC layer (dCCPC-lowE) as skylights. This radar chart is provided aiming to provide a comprehensive idea of how dCCPC-DB and dCCPC-lowE affects cooling and heating loads comparing with DB, that is, increase or decrease or stay same for different locations in different seasons. The quantity of thermal load variations were given in Fig. 10 in detail. For each radar chart, the labelled number from 1-12 represents the months from January to December throughout the year. The solid and dashed lines indicate the cooling and heating load of building with different skylights respectively. In general view, the locations can be categorized into three types, which are the locations where the building has cooling load only, has heating load only and has both cooling and heating loads. For the first type, the locations are Hong Kong, Miami, Bangkok and Manila. The cooling load provides obvious decreases especially in summer time when the skylights using the window with dCCPC layer. Due to the lower value of solar heat gain coefficient (SHGC), the low-E glazing with dCCPC (dCCPC-lowE) provides more reduction than the common double glazing with dCCPC (dCCPC-DB). For the locations with heating load only, e.g. Lhasa, Kiruna, Aberdeen, Birmingham and Helsinki, it can be found that the savings on heating load are not as much as on cooling load, even the heating load after using dCCPC window is more than that of using double glazing in some months. For the locations in which building needs cooling and heating, like Los Angeles, Rome, Beijing, Shanghai and Istanbul, similar results are obtained. The skylights with dCCPC layer can reduce cooling load in summer, and these reductions are quite much in some specific months and locations, for example, the July, August and September in Los Angeles, the July and August in Rome and Istanbul. Generally speaking, dCCPC and low-E coating can reduce cooling load effectively, but the low SHGC can also lead to the increase of heating load in cold seasons. Balances should be found to save the total energy consumption on both cooling and heating for building.

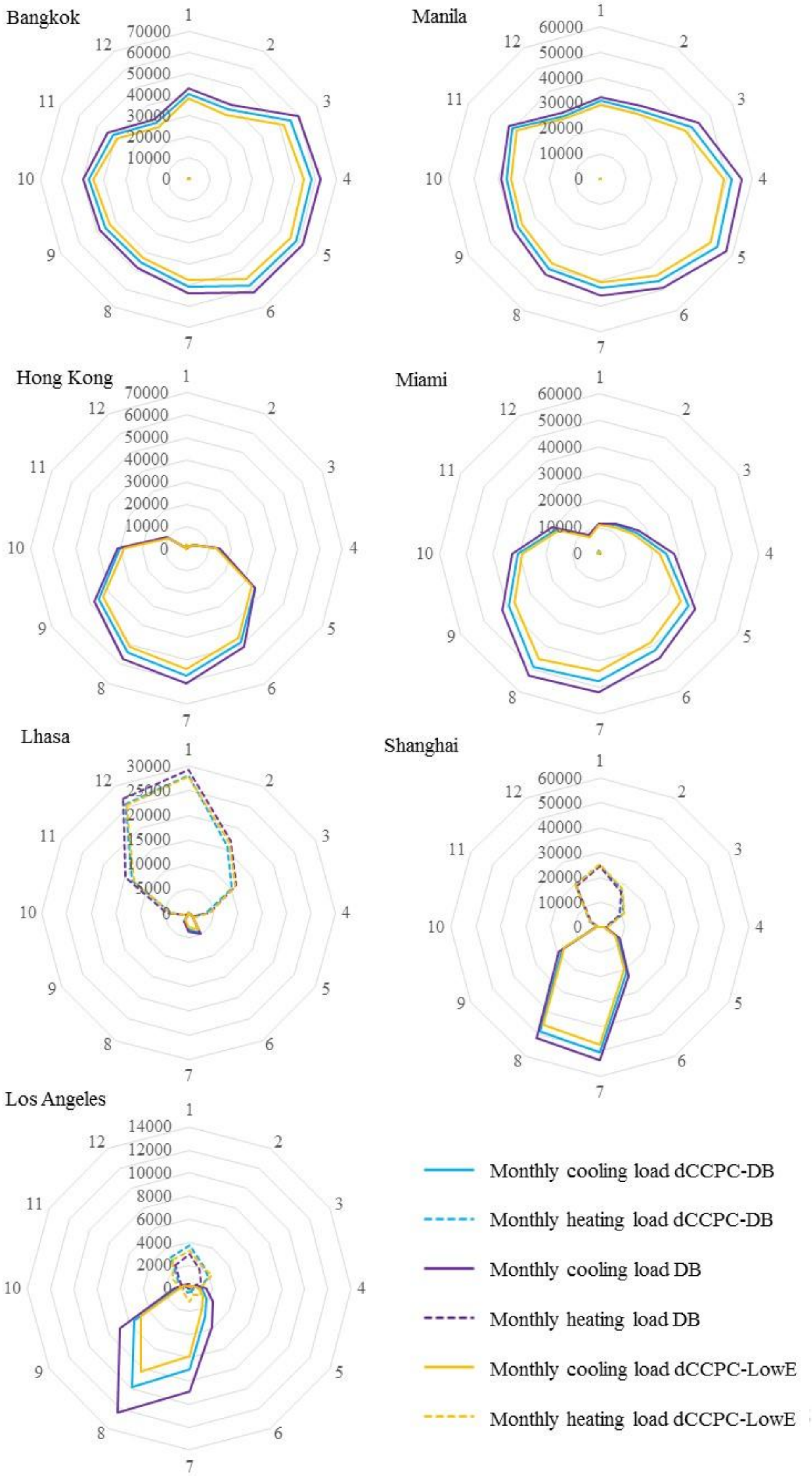

(a). for the latitude range of 13°N -34°N

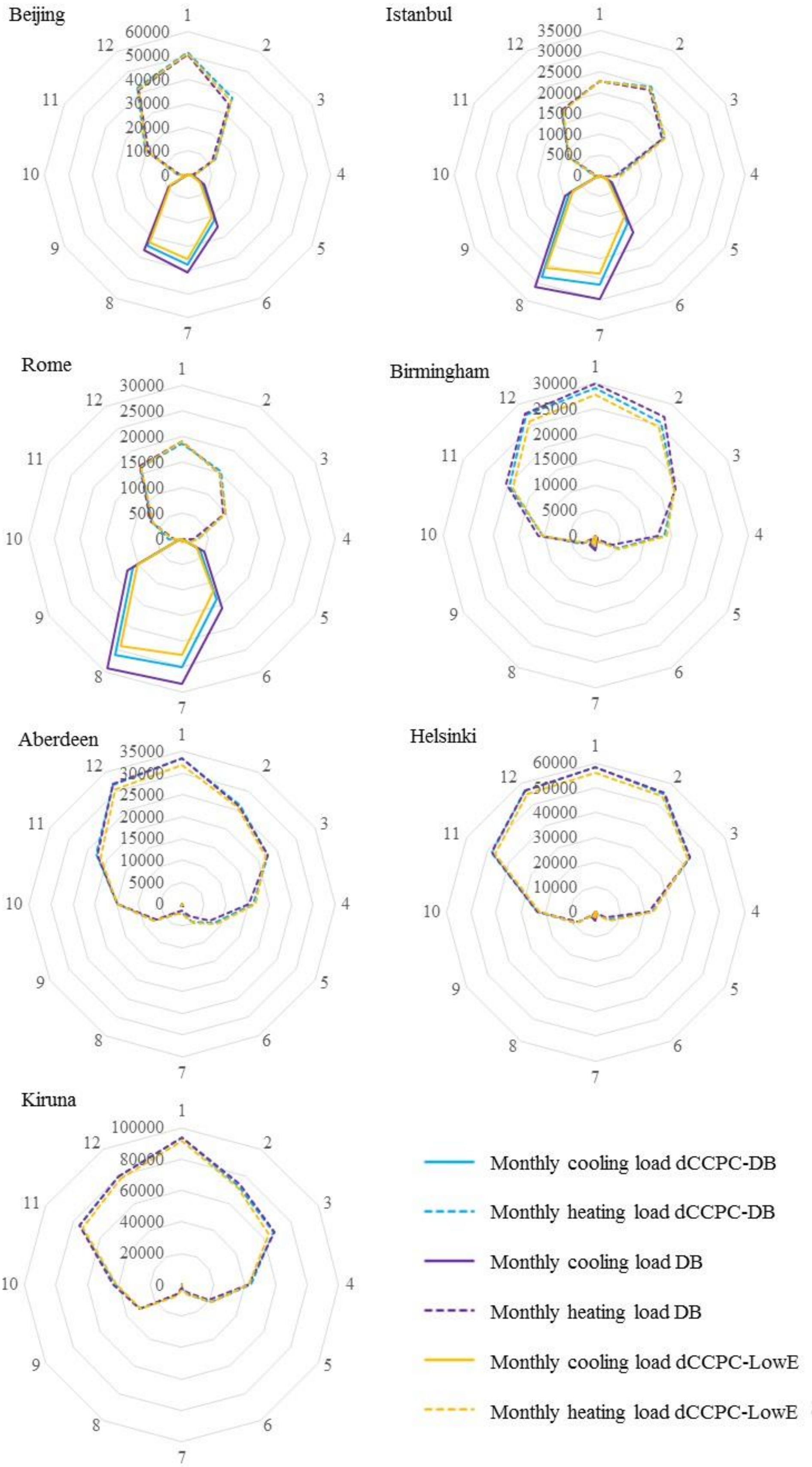

(b). for the latitude range of 34°N -68°N

Fig. 9. Monthly cooling and heating loads for the example building in 14 cities (Latitude: 13°N -68°N) with DB, dCCPC-DB and dCCPC-lowE as skylights, respectively

The annual thermal load for the sum of cooling and heating loads in the example building is summarized in Fig. 10, in which the effects of the skylights with dCCPC layer on the total thermal load are illustrated. The cities are arranged by climate category firstly. The climates are ordered from low to high altitude. In each climate type, the cities are ordered by the time percentage of clear sky from long to short. As is known from Fig. 9(a) and Fig. 9(b), the effects of dCCPC is mainly on reducing cooling load by preventing solar heat gain. On the contrary, it will also result in increasing heating load. Thus, after combining the variations on heating and cooling load, it provides different results compared to the result of either cooling or heating shown in Fig. 9(a) and Fig. 9(b). It was found that the thermal loads have slightly decreases (1%-3%) for the cold locations, like Helsinki, Kiruna and Aberdeen, which may be not suitable for using dCCPC. For the locations having cold winter, such as Beijing and Birmingham, heating takes more than half of the total thermal load, the reduction in thermal load by dCCPC are quite low (< 5%). In these locations, cold seasons are long and solar gain from window are expected to be as much as possible in winter to reduce heating load. It is important to point out that Lhasa is an exception among cold locations in which the thermal load of building is decreased after using dCCPC. Although most of the time during the whole year in Lhasa is cold, the clear sky takes about 65% of daytime during the whole year so that the annual solar radiation reaches 7.2GJ/m^2 which is extremely strong (Wu et al., 2015). Form the annual cooling load, it can be seen that using dCCPC-DB and dCCPC-lowE reduces 10% and 24% cooling load respectively compared to using traditional double glazing. They also lead to reductions in heating load in winter time. The reason is because the dCCPC layer causes lower transmittance of skylights so that more artificial lighting is required. The thermal energy from lighting offsets some requirements for heating. For the locations having long hot seasons, the window with dCCPC provides outstanding performance of reducing total thermal load. Use of dCCPC-lowE reduces up to 23% of annual thermal load compared with DB for Los Angeles, from 10% to 14% for Hong Kong, Rome, Miami, Bangkok and Manila. The reduction in heating and cooling load by dCCPC-DB also ranges from 5% to 10% for these locations.

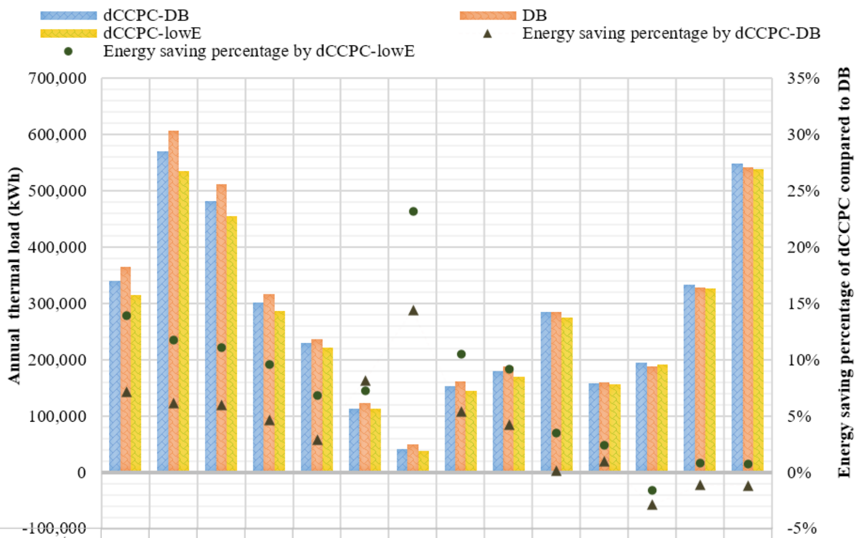

● Energy saving percentage by dCCPC-lowE	14%	12%	11%	10%	7%	7%	23%	10%	9%	3%	2%	-2%	1%	1%
▲ Energy saving percentage by dCCPC-DB	7%	6%	6%	5%	3%	8%	14%	5%	4%	0%	1%	-3%	-1%	-1%
City name	Miami	Bangkok	Manila	Hong Kong	Shanghai	Lhasa	Los Angeles	Rome	Istanbul	Beijing	Birmingham	Aberdeen	Helsinki	Kiruna

Fig. 10. Annual thermal load of the example building with dCCPC-DB, DB and dCCPC-lowE as skylights, respectively

4.3. Energy consumption of artificial lighting

Although dCCPC provides effective daylight control, when it is integrated with standard or low-E double glazing, its transmittance is smaller than that of traditional double glazing. Thus, more artificial lighting may be required to guarantee the indoor illuminance level. The annual electricity demand of artificial lighting is demonstrated in Fig. 11, together with the percentage of relative difference of lighting consumption between using dCCPC-DB and DB as skylights. Because the difference in the amount of annual lighting energy consumptions between using dCCPC-DB and dCCPC-lowE for each city is quite small and less than 3%, the percentage difference of using dCCPC-lowE is not shown in Figure. It can be seen that the lighting energy consumption is increased by about 6% when using the skylights with dCCPC layer in general, except for Beijing. It has been discussed that dCCPC has the advantage of diffusing incident light. When the sun is in lower position, traditional double glazing cannot provide a relatively large bright-area, but the dCCPC could lit larger space through diffusing. In Beijing, the sky conditions are possible to be intermediate or clear when the sun is low, and less lighting is needed when the dCCPC is used. For the locations with lower solar radiation and longer time of overcast sky, i.e. the time of overcast and overcast to intermediate sky is more than 80%, for instance, Helsinki, Birmingham, Kiruna and Aberdeen, dCCPC causes relatively large increase on the demand of artificial lighting. The results also demonstrate that Hong Kong is an exception of the cities located in low latitude. Utilizing dCCPC causes 19% increase of lighting energy consumption. The reason is because Hong Kong has the opposite condition with Beijing: during the time when sun is low, more of the sky conditions in Hong Kong is likely to be overcast, and light is prevented by dCCPC causing much more demand on lighting. It is also important to mention another exception of Lhasa. Lhasa has strong direct sunlight and long-time clear sky conditions (about 65%). Although the outdoor illuminance will be extremely high sometime, e.g. 90klux, it is still rare case. Thus, dCCPC performs low transmittance, e.g. 0.3-0.4, during these time periods so that much more lighting is needed. However, shading requirement is not considered in this simulation. But it can be speculated that the normal double glazing can provide extreme bright indoor environment as well as the very high indoor illuminance level in Lhasa, and shading should be a necessary requirement to provide a comfort visual environment. The energy consumed by artificial lighting should be larger than the results presented under such circumstances.

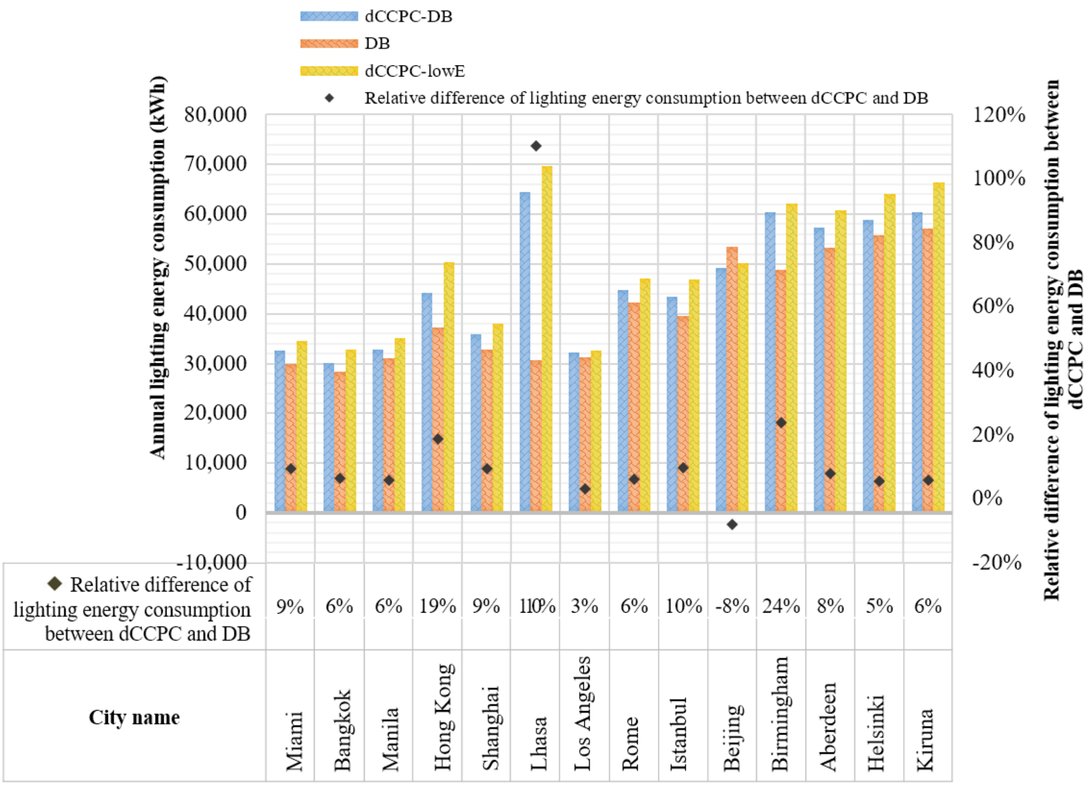

Fig. 11. Annual lighting energy consumption of the example building with dCCPC-DB, DB and dCCPC-lowE as skylights, respectively

The energy consumption of a building mainly consists of electricity usage of artificial lighting, electricity usage of equipment and energy consumption of heating and cooling system. As discussed in previous sections, dCCPC can reduce total thermal load but increase lighting usage, and the variation of lighting caused by dCCPC can also lead to the change of thermal load. It is important to investigate the interactions among different energy usage sectors. In the energy simulations in this study, it is assumed that all of the systems and schedules are same. Thus the electricity usage of equipment is assumed to be same for different locations. The lighting and heating/cooling energy demands are the only two aspects that should be considered to evaluate the performance of using the dCCPC skylights. Fig. 12 shows the comparisons of the total energy consumptions of lighting, cooling and heating when utilizing DB, dCCPC-DB and dCCPC-lowE as skylights. It can be found that for the locations with long hot seasons such as Los Angeles, Miami, Bangkok and Manila, a considerable reductions of up to 13% (dCCPC-lowE) and 8% (dCCPC-DB) occur in total energy consumption. A small reduction of 1%-5% can be obtained by utilizing dCCPC for the locations having temperate and continental climates, e.g. Beijing, Shanghai, Rome, Istanbul and Hong Kong. For the locations having long cold seasons like Birmingham, Aberdeen, Helsinki and Kiruna, the reduction in solar gain by dCCPC leads to more energy consumption in heating load and artificial lighting.

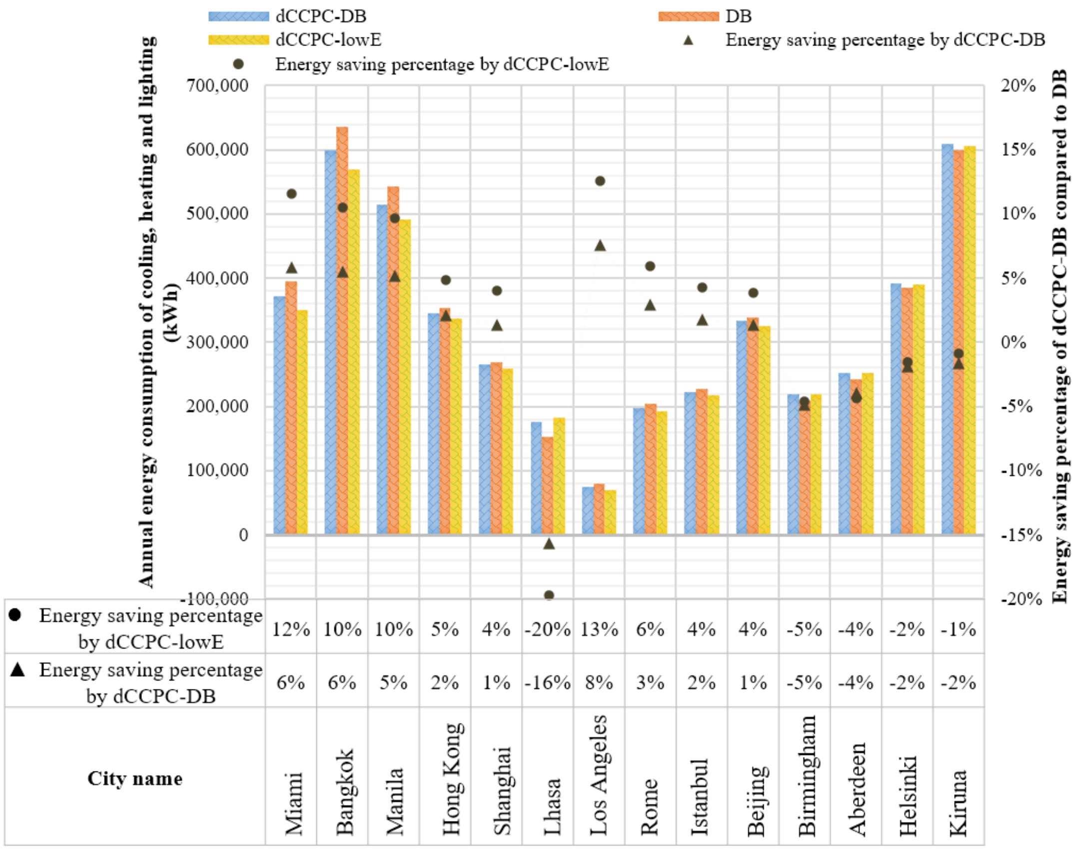

Fig. 12. Annual energy consumption of cooling, heating and lighting for the example building with dCCPC-DB, DB and dCCPC-lowE as skylights, respectively

4.4. Model validation and discussion

To input to the building energy simulation in this study, the variable transmittance of the studied skylights, dCCPC-DB and dCCPC-lowE, were according to the sky condition and solar angles of given time and location using the pre-determined mathematical model (Tian and Su, 2018a) and daylight simulation in Grasshopper. An experiment was taken to validate the accuracy of this part of simulation model calculating the variable transmittance of dCCPC skylight panels. The experiment was conducted in Hefei, China (N 31°N, 117°E) for a dCCPC element with a tilt angle of 8° facing south. The measurement was taken from 9:10am to 12:00pm on 20th Sep under a changing sky condition between typical overcast sky, intermediate sky and clear sky.

Table 4 demonstrates the values of simulation and measured results of dCCPC skylights under different sky conditions. It was found that almost all of the deviations between experiment and simulation results are smaller than 10%, only the deviation at 10:50am are about 16% which may be caused by the occasional experimental error. The root-mean-square-error (RMSE) of the two data sets are 3.33% and 2.89% respectively, which are quite small and can prove the precision and reliability of the transmittance prediction model.

Table 4. Validation of transmittance prediction for dCCPC skylights in building energy simulation

Local time	Sky condition	dCCPC-double glazing (dCCPC-DB)			dCCPC-lowE		
		Experiment results	Simulation results	Errors	Experiment results	Simulation results	Errors
9:10	overcast	0.51	0.51	1.6%	0.45	0.44	1.2%
9:20	intermediate	0.63	0.57	10.8%	0.55	0.50	10.4%
9:30	overcast	0.58	0.55	6.7%	0.51	0.48	6.3%
9:40	overcast	0.54	0.51	5.3%	0.47	0.45	4.9%
9:50	clear	0.56	0.57	2.4%	0.48	0.50	2.8%
10:00	clear	0.55	0.52	4.7%	0.48	0.46	4.3%
10:10	clear	0.53	0.51	3.0%	0.46	0.45	2.6%
10:20	clear	0.50	0.51	2.8%	0.43	0.45	3.2%
10:30	intermediate	0.47	0.51	7.1%	0.41	0.44	7.5%
10:40	intermediate	0.42	0.47	9.6%	0.37	0.41	10.0%
10:50	clear	0.46	0.40	16.1%	0.40	0.35	15.6%
11:00	clear	0.36	0.37	1.8%	0.32	0.32	2.1%
11:10	clear	0.39	0.40	4.1%	0.34	0.35	4.4%
11:20	clear	0.31	0.33	5.7%	0.27	0.29	6.0%
11:30	overcast	0.45	0.50	9.1%	0.39	0.43	9.5%
11:40	overcast	0.45	0.49	7.9%	0.39	0.43	8.2%
11:50	intermediate	0.47	0.46	1.6%	0.41	0.40	1.2%
12:00	clear	0.38	0.35	10.0%	0.33	0.30	9.6%
RMSE		3.33%			2.89%		

This paper aims to provide an idea of the feasibility of using dCCPC panel as skylights in different locations with various climates, with a focus to show how the proposed mathematical model of transmittance can be incorporated in a building energy simulation. Therefore the office building used for simulation in this study is assumed to be a typical single-story air-conditioned building according to the CIBSE Guide (CIBSE, 2000), which is expected to be a benchmark office building to show the overall effect of dCCPC skylights on building energy consumption.

The energy simulation of building was initiated from Grasshopper which integrates several popular simulation engines such as EnergyPlus, Radiance and Daysim. The accuracy of these simulation software packages has been verified in many studies. EnergyPlus is a famous tool for simulating energy consumption of building, developed by the US Department of Energy and released in 2001. In recent decades, many researchers (Tabares-Velasco et al., 2012, Mateus et al., 2014, Sang et al., 2017, Zhang et al., 2018, Rhodes et al., 2015) have used and validated this software in their works related to building energy. The availability and reliability of EnergyPlus has been highlighted and proved. For example, Anđelković et al. (Anđelković et al., 2016) proceeded a long term research to validate the reliability of EnergyPlus by comparing the simulation and experiment results in surface temperature, air temperature and air velocity. The results highlight a very good agreement and high-level matching between simulation and measured results. In the study provided by Dahanayake and Chow (Dahanayake and Chow, 2017) who investigated the energy performance of a building with vertical greenery systems, the results provided by EnergyPlus also shows a good agreement with experiment results. In the research provided by Shabunko et al. (Shabunko et al., 2018), they compared the energy consumptions of three types of real buildings and their simulation models. The RMSE value of energy use intensity falls below 7% of simulation models which proved the good accuracy of EnergyPlus in providing engineering models to predict building energy consumption. Radiance is a versatile tool for lighting simulation and a physically based renders with available source code, which is a highly accurate ray-tracing software for UNIX computers (BerkeleyLab). The simulation utilize a backwards ray-tracing method with extensions to solve the rendering equation efficiently under most conditions (Ward). Daysim is a Radiance-based simulation tool for analysing the daylighting, shading and lighting control system in building (Jakubiec and Reinhart, 2012). There are many studies validated their accuracy in lighting simulation (Grobe, 2018, Kim et al., 2018, Pagliolico et al., 2017, Mangkuto et al., 2016, Manzan, 2014, Dabe and Adane, 2018). In the research provided by Jakubiec and Reinhart (Jakubiec and Reinhart, 2013), the errors of simulation and test results range between 3.6% and 5.3% when investigating the annual urban irradiation by Daysim. Yun and Kim (Yun and Kim, 2013) used EnergyPlus and Daysim to validate the lighting energy consumption of a building, and found that Daysim provides quite close values of lighting power fraction and lighting energy consumption with measured results. Su et al. (Su et al., 2012) simulated the optical performance of lens-walled CPC in ray tracing, flux distribution and optical efficiency by Radiance. The results are compared with the results by the commercial optical analysis software Photopia, and the average relative difference between them is within 5%. Acosta et al. (Acosta et al., 2015) proposed that Daysim shows the sufficient accuracy to obtain credible results as a lighting simulation program after comparing several different lighting simulation software based on the test cases established by the CIE (CIE, 2006).

As described above, the proposed mathematical model of transmittance for dCCPC skylights was validated in an outdoor experiment with a good accuracy, and also those building energy simulation software packages have proved accurate enough, therefore, incorporation of the proposed mathematical model in the building energy simulation software can offer a cost effective way to evaluate the viability of dCCPC skylights in buildings. It will be ideal to be followed by the field test of dCCPC skylights in a real building, but due to the resource constriction, it is a regret that a corresponding experiment was unable to be implemented in the current study. However, it is expected and recommended to proceed this field test in a further work.

5. Conclusion and recommendation

Considering the daylighting control feature of a miniature dielectric crossed compound parabolic concentrator (dCCPC) panel, this study has investigated its effects in terms of energy saving by simulating an example office building with dCCPC panel as skylights. In order to do this, calculation of variable transmittance of dCCPC panel has been introduced in an innovative way by using a multiple nonlinear regression model and definition of equivalent altitude and azimuth angles for a tilted surface. In particular, Grasshopper has been used to programme this model and link it to building energy simulation. To evaluate the suitability of dCCPC panels for different locations, 14 cities in the northern hemisphere with the latitude ranging from 13° to 67° have been selected for simulation study. Three types of skylights are compared, which are standard double glazing (DB), double glazing with dCCPC layer (dCCPC-DB), and double glazing with dCCPC layer and low-E coating (dCCPC-lowE).

The key findings of this paper can be summarized into following points:

1) In general, dCCPC panel as skylights can reduce cooling load due to effectively mitigating solar heat gain. However, it also causes increases of heating load and artificial lighting energy consumption. The energy performance of a building with dCCPC skylights is also related to the local climate conditions such as solar irradiation and temperature.

2) The dCCPC skylight is more suitable for the cities having long summer time, such as Bangkok, Manila, Miami, and Los Angeles. The reduction of thermal load is up to 23% and the total energy saving could reach 13%.

3) The dCCPC skylight is more effective under clear sky conditions. For example, Los Angeles (23% reduction of thermal load) is the best choice for using dCCPC due to its longest period of clear sky among the cities with long hot seasons.

4) For the cities with continental climates, only the place with prevalent clear sky is appropriate for using dCCPC skylight. For instance, in Beijing, Rome, Hong Kong and Shanghai, dCCPC could decrease the annual thermal load by 3% to 10%. Considering the lighting energy consumption, the total energy saving ranges from 1% to 5% in these cities.

5) The dCCPC skylight is not suitable for the cities with long cold seasons, e.g. Aberdeen, Birmingham, Helsinki and Kiruna. The reduction of solar gain by dCCPC leads to more energy consumption in heating load and artificial lighting. Using dCCPC in these cities leads to 1%-5% increase of total annual energy consumption.

6) In terms of optical properties, dCCPC is recommended for all locations for the purpose of glare control, especially for the cities with strong solar radiation.

The further work about dCCPC is suggested to be proceeded in the following aspects. Firstly, different shading devices should be considered and glare analysis are recommended to be taken to evaluate the dCCPC effects on indoor visual environment comparing with traditional glazing, and then the energy analysis in this study could be updated by considering various shading devices. Secondly, an experiment implemented in a real building was highly recommended to verify the simulated effect of dCCPC skylight on building energy and visual environment. Thirdly, considering the great potential of utilizing dCCPC as skylights in diffusing direct sunlight and energy saving of building, the asymmetric dCCPC is suggested for investigating its feasibility in daylighting control as vertical building facade. Finally, the economic analysis of dCCPC could be taken to evaluate its viability in practical application.

Acknowledgements

The authors would like to thank the European Commission for the Marie Skłodowska-Curie Fellowship grants (H2020-MSCA-IF-2014-658217, H2020-MSCA-IF-2015-703746). We would also like to thank Dr. Mark Jongewaard from Photopia for creating intermediate sky models for this study.

Reference

ACOSTA, I., MU OZ, C., ESQUIVIAS, P., MORENO, D. & NAVARRO, J. 2015. Analysis of the accuracy of the sky component calculation in daylighting simulation programs. *Solar Energy,* 119**,** 54-67.

ACUITYBRANDS. n.d. *Indoor Prismatic Skylights* [Online]. Acuity Brands Lightring, Inc. Available: https://www.acuitybrands.com/products/lighting/indoor/skylights#t=Products&f:@flightingproducttype51681=[Skylight] [Accessed 23rd Jun 2018].

AHADI, A. A., SAGHAFI, M. R. & TAHBAZ, M. 2017. The study of effective factors in daylight performance of light-wells with dynamic daylight metrics in residential buildings. *Solar Energy,* 155**,** 679-697.

ANĐELKOVIĆ, A. S., MUJAN, I. & DAKIĆ, S. 2016. Experimental validation of a EnergyPlus model: Application of a multi-storey naturally ventilated double skin façade. *Energy and Buildings,* 118**,** 27-36.

ATTIA, S., HAMDY, M. & EZZELDIN, S. 2017. Twenty-year tracking of lighting savings and power density in the residential sector. *Energy and Buildings,* 154**,** 113-126.

BAIG, H., SARMAH, N., CHEMISANA, D., ROSELL, J. & MALLICK, T. K. 2014. Enhancing performance of a linear dielectric based concentrating photovoltaic system using a reflective film along the edge. *Energy,* 73**,** 177-191.

BERKELEYLAB. *Radiance* [Online]. Available: http://radsite.lbl.gov/radiance/framew.html [Accessed 2/15 2016].

CIBSE 2000. Energy consumption guide 19: energy use in offices.

CIE 2006. Test cases to assess the accuracy of lighting computer programs. Commission Internationale de l'Éclairage.

DABE, T. J. & ADANE, V. S. 2018. The impact of building profiles on the performance of daylight and indoor temperatures in low-rise residential building for the hot and dry climatic zones. *Building and Environment,* 140**,** 173-183.

DAHANAYAKE, K. W. D. K. C. & CHOW, C. L. 2017. Studying the potential of energy saving through vertical greenery systems: Using EnergyPlus simulation program. *Energy and Buildings,* 138**,** 47-59.

DUBOIS, M.-C. & BLOMSTERBERG, Å. 2011. Energy saving potential and strategies for electric lighting in future North European, low energy office buildings: A literature review. *Energy and Buildings,* 43**,** 2572-2582.

ENERGYPLUS 2017. Energyplus version 8.8.0 documentation-engineering reference. U.S. Department of Energy.

ENERGYPLUS. n.d. *EnergyPlus Weather Data* [Online]. National Renewable Energy Laboratory (NREL). Available: https://energyplus.net/weather [Accessed 5/21 2017].

EWC. n.d. *Windows for high-performance commercial buildings* [Online]. Available: http://www.commercialwindows.org/shgc.php [Accessed 12th Oct 2017].

EXCELITE. n.d. *Prismatic sheet* [Online]. Excelite Ltd. Available: https://www.exceliteplas.com/product/prismatic-sheet/ [Accessed 23rd Jun 2018].

GOIA, F. 2016. Search for the optimal window-to-wall ratio in office buildings in different European climates and the implications on total energy saving potential. *Solar Energy,* 132**,** 467-492.

GOIA, F., HAASE, M. & PERINO, M. 2013. Optimizing the configuration of a façade module for office buildings by means of integrated thermal and lighting simulations in a total energy perspective. *Applied Energy,* 108**,** 515-527.

GRASSHOPPER. n.d. *Grasshopper - algorithmic modeling for rhino* [Online]. Available: http://www.grasshopper3d.com/ [Accessed 5th Oct 2017].

GROBE, L. O. 2018. Characterization and data-driven modeling of a retro-reflective coating in Radiance. *Energy and Buildings,* 162, 121-133.

HOURANI, M. M. & HAMMAD, R. N. 2012. Impact of daylight quality on architectural space dynamics: Case study: City Mall – Amman, Jordan. *Renewable and Sustainable Energy Reviews,* 16, 3579-3585.

HRASKA, J. 2015. Chronobiological aspects of green buildings daylighting. *Renewable Energy,* 73, 109-114.

JAKUBIEC, J., A. & REINHART, C., F. 2012. *Overview and inroduction to DAYSIM and current research developments* [Online]. Available: https://www.radiance-online.org//community/workshops/2012-copenhagen/Day1/Jakubiec/jakubiec,reinhart_radiance-workshop-presentation_daysim.pdf [Accessed 8th Oct 2017].

JAKUBIEC, J. A. & REINHART, C. F. 2013. A method for predicting city-wide electricity gains from photovoltaic panels based on LiDAR and GIS data combined with hourly Daysim simulations. *Solar Energy,* 93, 127-143.

KIM, D., COX, S. J., CHO, H. & YOON, J. 2018. Comparative investigation on building energy performance of double skin façade (DSF) with interior or exterior slat blinds. *Journal of Building Engineering,* 20, 411-423.

KINGSPAN. n.d. *Quasar prismatic skylight* [Online]. CADdetails. Available: https://www.caddetails.com/Main/Company/ViewProduct?productID=13075&companyID=2988&isFeatured=False&currentTab=Product [Accessed 23rd Jun 2018].

LI, G. 2018. Design and development of a lens-walled compound parabolic concentrator-a review. *Journal of Thermal Science*, 1-13.

LI, G., XUAN, Q., ZHAO, X., PEI, G., JI, J. & SU, Y. 2018. A novel concentrating photovoltaic/daylighting control system: Optical simulation and preliminary experimental analysis. *Applied Energy*, 228, 1362-1372.

LIBERMAN, J. 1990. *Light Medicine of the Future,* New Mexico, Bear & Company.

LIGHTINGRESEARCHCENTER. n.d. *Reflectance* [Online]. Available: http://www.lrc.rpi.edu/education/learning/terminology/reflectance.asp [Accessed 21st Sep 2017].

LOWRY, G. 2016. Energy saving claims for lighting controls in commercial buildings. *Energy and Buildings,* 133, 489-497.

MALLICK, T. K. & EAMES, P. C. 2007. Design and fabrication of low concentrating second generation PRIDE concentrator. *Solar Energy Materials and Solar Cells,* 91, 597-608.

MALLICK, T. K., EAMES, P. C., HYDE, T. J. & NORTON, B. 2004. The design and experimental characterisation of an asymmetric compound parabolic photovoltaic concentrator for building façade integration in the UK. *Solar Energy,* 77, 319-327.

MALLICK, T. K., EAMES, P. C. & NORTON, B. 2006. Non-concentrating and asymmetric compound parabolic concentrating building façade integrated photovoltaics: An experimental comparison. *Solar Energy,* 80, 834-849.

MANGKUTO, R. A., ASRI, A. D., ROHMAH, M., NUGROHO SOELAMI, F. X. & SOEGIJANTO, R. M. 2016. Revisiting the national standard of daylighting in Indonesia: A study of five daylit spaces in Bandung. *Solar Energy,* 126, 276-290.

MANZAN, M. 2014. Genetic optimization of external fixed shading devices. *Energy and Buildings,* 72, 431-440.

MATEUS, N. M., PINTO, A. & GRA A, G. C. D. 2014. Validation of EnergyPlus thermal simulation of a double skin naturally and mechanically ventilated test cell. *Energy and Buildings,* 75, 511-522.

PAGLIOLICO, S. L., VERSO, V. R. M. L., BOSCO, F., MOLLEA, C. & LA FORGIA, C. 2017. A Novel Photo-bioreactor Application for Microalgae Production as a Shading System in Buildings. *Energy Procedia,* 111, 151-160.

PEREZ, R., INEICHEN, P., SEALS, R., MICHALSKY, J. & STEWART, R. 1990. Modeling daylight availability and irradiance components from direct and global irradiance. *Solar Energy,* 44**,** 271-289.

PVEDUCATION. n.d. *Spectral Response* [Online]. PVEDUCATION.ORG. Available: http://www.pveducation.org/pvcdrom/solar-cell-operation/spectral-response [Accessed 4th Feb 2018].

RADIANCE 2014. The RADIANCE 4.2 synthetic imaging system. Berkeley: Lawrence Berkeley Laboratory.

RHINOCEROS. n.d. *Rhino 5 Features* [Online]. Available: https://www.rhino3d.com/eu/ [Accessed 5th Oct 2017].

RHODES, J. D., GORMAN, W. H., UPSHAW, C. R. & WEBBER, M. E. 2015. Using BEopt (EnergyPlus) with energy audits and surveys to predict actual residential energy usage. *Energy and Buildings,* 86**,** 808-816.

S. R. KELLERT, J. HEERWAGEN & MADOR, M. 2008. *Biophilic Design: The Theory Science and Practice of Bringing Buildings to Life*, John Wiley & Sons.

SANG, Y., ZHAO, J. R., SUN, J., CHEN, B. & LIU, S. 2017. Experimental investigation and EnergyPlus-based model prediction of thermal behavior of building containing phase change material. *Journal of Building Engineering,* 12**,** 259-266.

SARMAH, N. & MALLICK, T. K. 2015. Design, fabrication and outdoor performance analysis of a low concentrating photovoltaic system. *Solar Energy,* 112**,** 361-372.

SARMAH, N., RICHARDS, B. S. & MALLICK, T. K. 2014. Design, development and indoor performance analysis of a low concentrating dielectric photovoltaic module. *Solar Energy,* 103**,** 390-401.

SHABUNKO, V., LIM, C. M. & MATHEW, S. 2018. EnergyPlus models for the benchmarking of residential buildings in Brunei Darussalam. *Energy and Buildings,* 169**,** 507-516.

SHC 2015. Newsletter 1: Overview and first results. *SHC Task 50.*

SIVAJI, A., SHOPIAN, S., NOR, Z. M., CHUAN, N.-K. & BAHRI, S. 2013. Lighting does Matter: Preliminary Assessment on Office Workers. *Procedia - Social and Behavioral Sciences,* 97**,** 638-647.

SU, Y., PEI, G., RIFFAT, S. B. & HUANG, H. 2012. Radiance/Pmap simulation of a novel lens-walled compound parabolic concentrator (lens-walled CPC). *Energy Procedia,* 14**,** 572-577.

TABARES-VELASCO, P. C., CHRISTENSEN, C. & BIANCHI, M. 2012. Verification and validation of EnergyPlus phase change material model for opaque wall assemblies. *Building and Environment,* 54**,** 186-196.

TIAN, M. & SU, Y. 2015. A study on use of three-dimensional miniature dielectric compound parabolic concentrator (3D dCPC) for daylighting control application. *14th International Conference on Sustainable Energy Technologies -SET 2015.* Nottingham, UK.

TIAN, M. & SU, Y. 2016. three dimensional dielectric compound parabolic concentrator (3D dCPC) for daylighting control in roofing. *11th Conference on Advanced Building Skins.* Bern, Switzerland.

TIAN, M. & SU, Y. 2018a. Multiple nonlinear regression model for predicting the optical performances of dielectric Crossed Compound Parabolic Concentrator (dCCPC). *Sol. Energy*, 159**,** 212-225.

TIAN, M. & SU, Y. 2018b. Visual performance of building with dielectric crossed compound parabolic concentrator (dCCPC) panel as skylights. *17th International conference on sustainable energy technologies.*

TIAN, M., SU, Y., ZHENG, H., PEI, G., LI, G. & RIFFAT, S. 2017. A review on the recent research progress in the compound parabolic concentrator (CPC) for solar energy applications. *Renewable and Sustainable Energy Reviews*.

ULAVI, T., HEBRINK, T. & DAVIDSON, J. H. 2014a. Analysis of a Hybrid Solar Window for Building Integration. *Energy Procedia,* 57**,** 1941-1950.

ULAVI, T., HEBRINK, T. & DAVIDSON, J. H. 2014b. Analysis of a hybrid solar window for building integration. *Solar Energy,* 105**,** 290-302.

WALZE, G., NITZ, P., ELL, J., GEORG, A., GOMBERT, A. & HOSSFELD, W. 2005. Combination of microstructures and optically functional coatings for solar control glazing. *Solar Energy Materials and Solar Cells,* 89**,** 233-248.

WARD, G. J. *The RADIANCE Lighting Simulation and Rendering System* [Online]. Lawrence Berkeley Laboratory. Available: http://radsite.lbl.gov/radiance/papers/sg94.1/Siggraph1994a.pdf.

WONG, I. L. 2017. A review of daylighting design and implementation in buildings. *Renewable and Sustainable Energy Reviews,* 74**,** 959-968.

WU, M., LIU, X. & TANG, H. 2015. Simulation Analysis on the Solar Heating System Combined with Tabs in Lhasa, China of Annex 59. *Energy Procedia,* 78**,** 2439-2444.

YU, X., SU, Y., ZHENG, H. & RIFFAT, S. 2014. A study on use of miniature dielectric compound parabolic concentrator (dCPC) for daylighting control application. *Building and Environment,* 74**,** 75-85.

YUN, G. & KIM, K. S. 2013. An empirical validation of lighting energy consumption using the integrated simulation method. *Energy and Buildings,* 57**,** 144-154.

ZACHAROPOULOS, A., EAMES, P. C., MCLARNON, D. & NORTON, B. 2000. Linear dielectric non-imaging concentrating covers for PV integrated building facades. *Solar Energy,* 68**,** 439-452.

ZHANG, L., ZHANG, R., HONG, T., ZHANG, Y. & MENG, Q. 2018. Impact of post-rainfall evaporation from porous roof tiles on building cooling load in subtropical China. *Applied Thermal Engineering,* 142**,** 391-400.

Figure

Figures

Figure 1

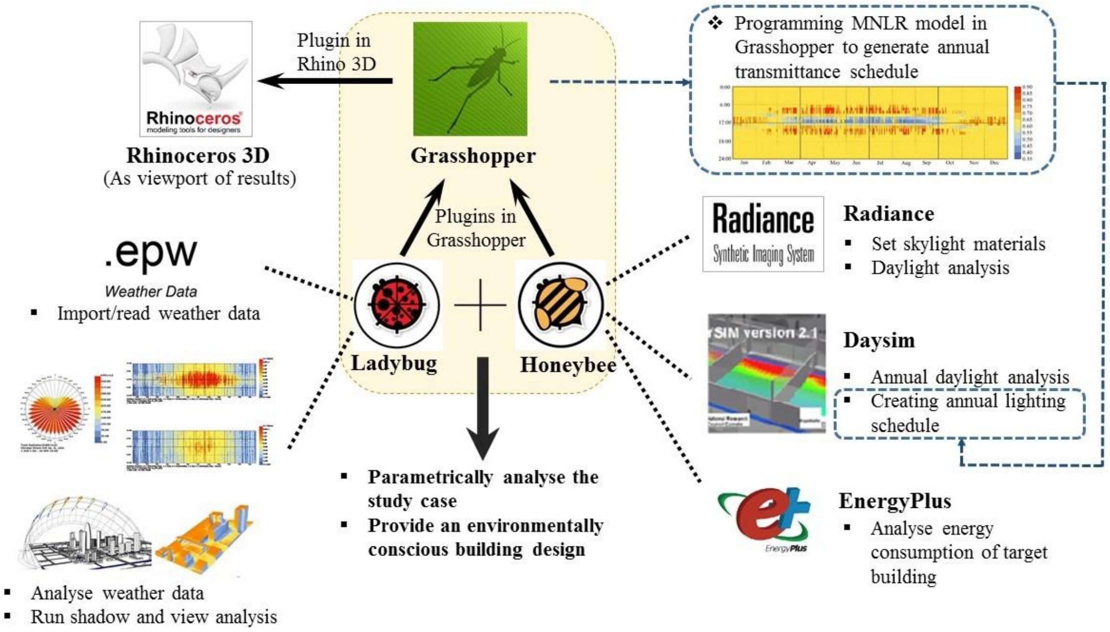

Figure 2

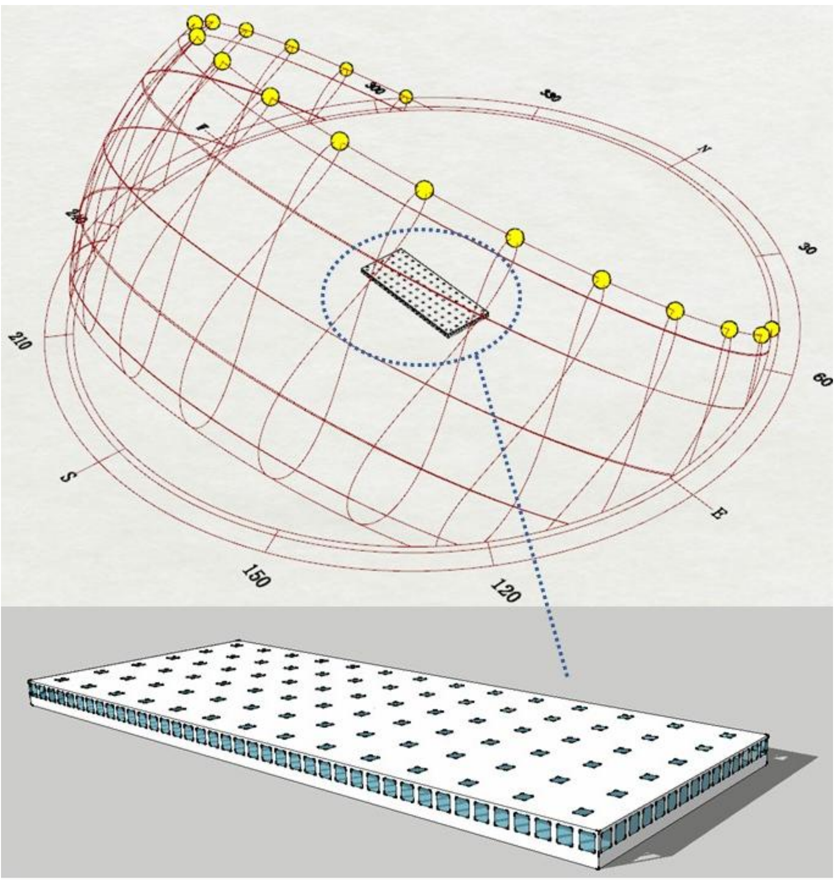

Figure 3

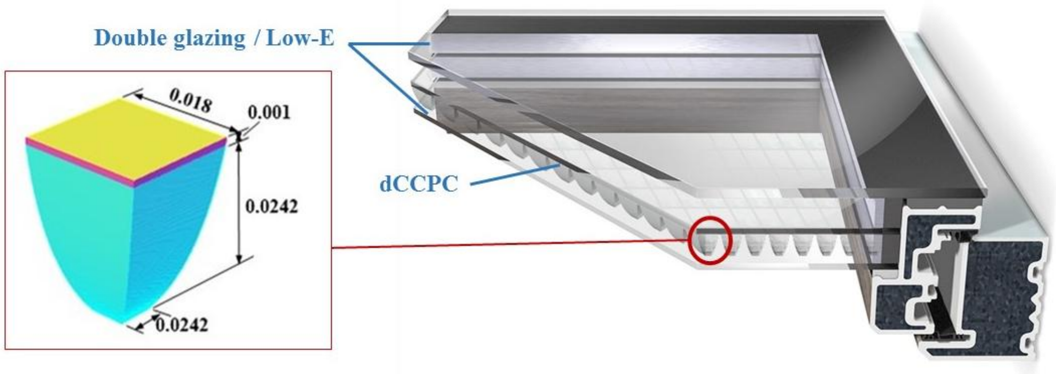

Figure 4

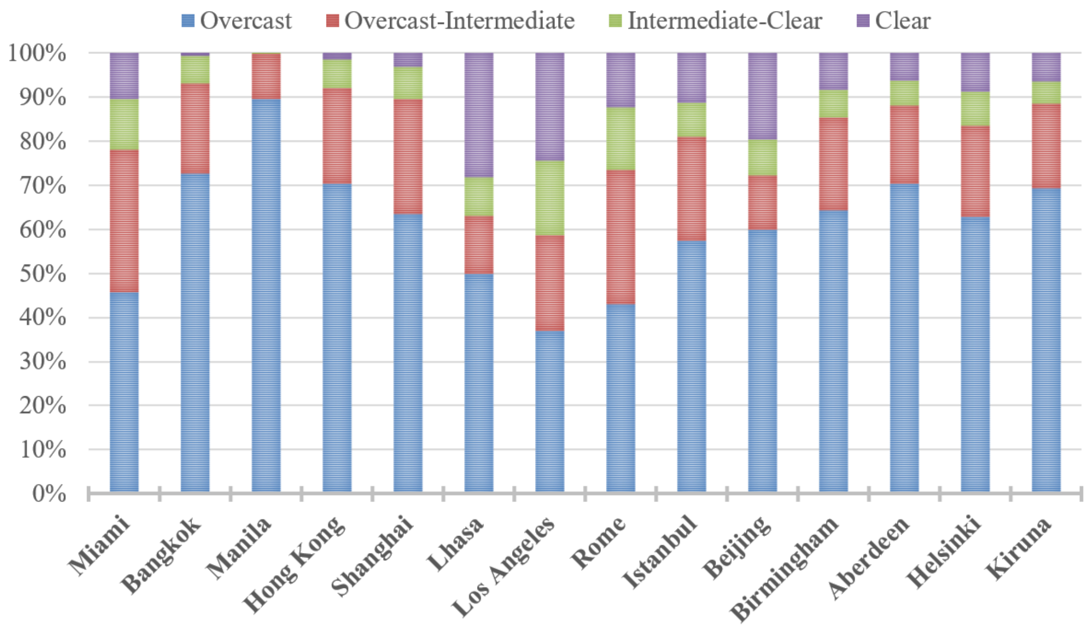

Figure 5

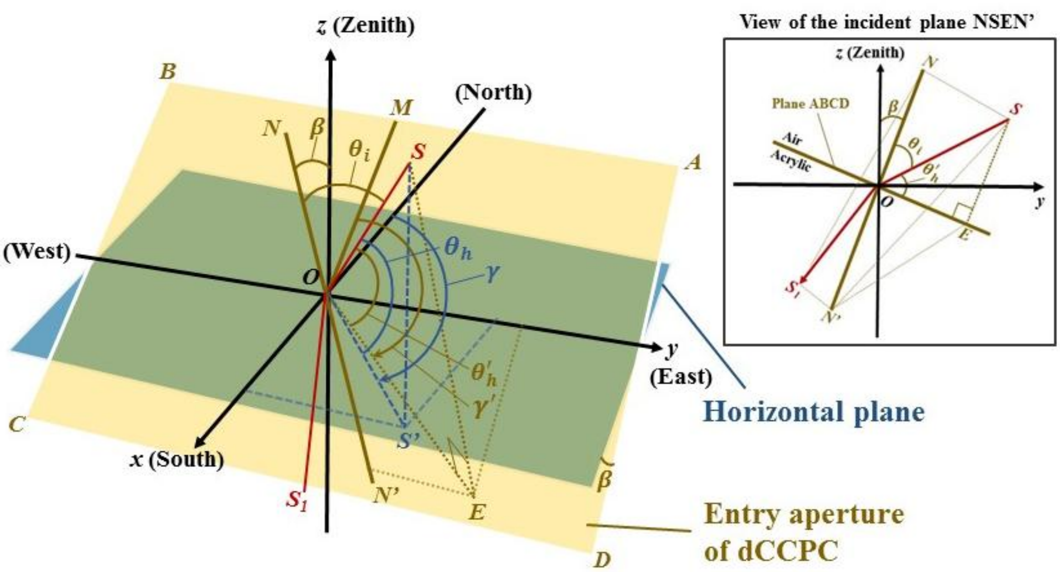

Figure 6

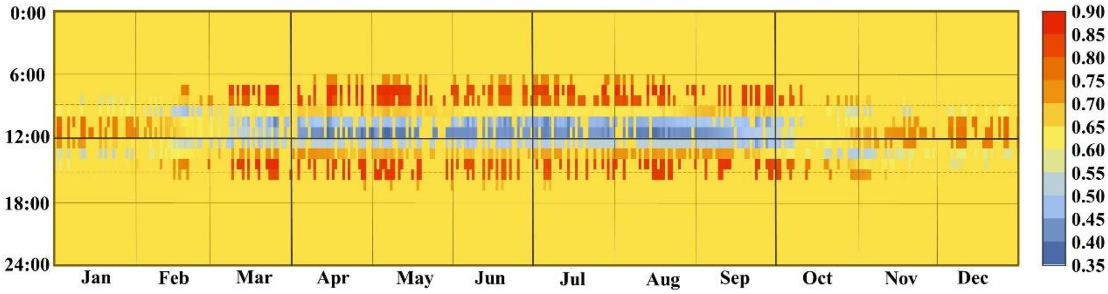

Figure 7

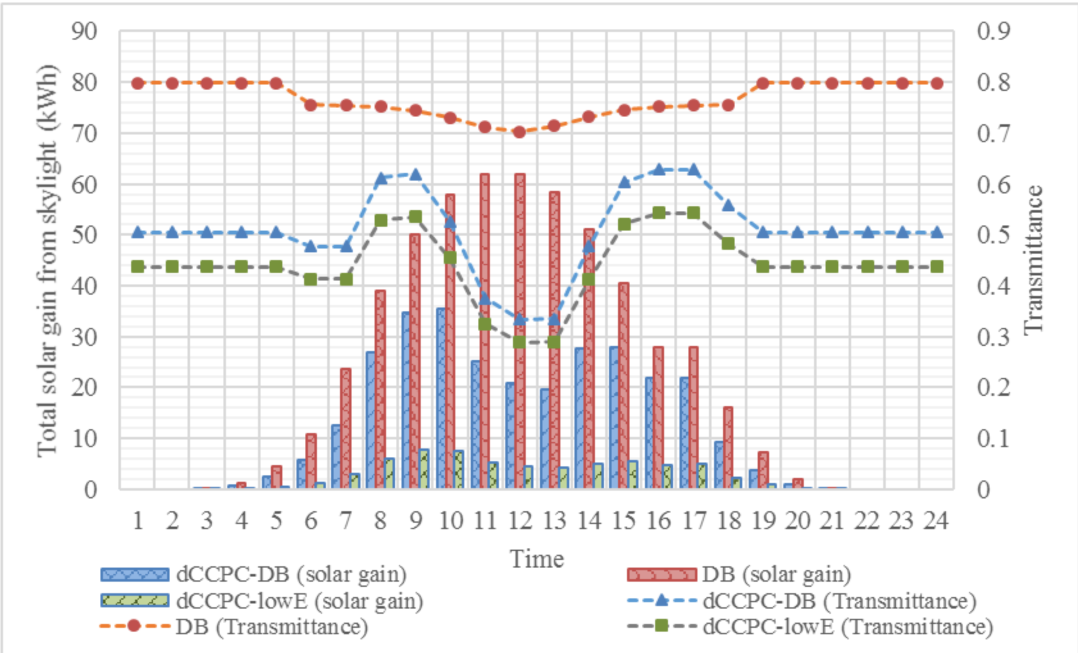

Figure 8

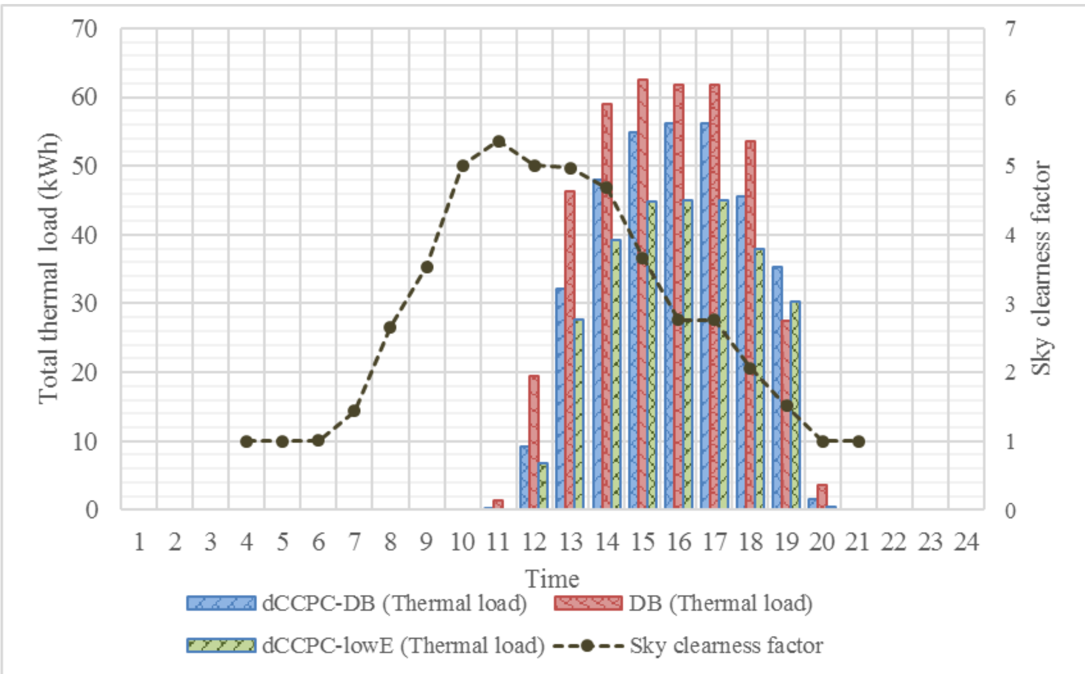

Figure 9 (a)

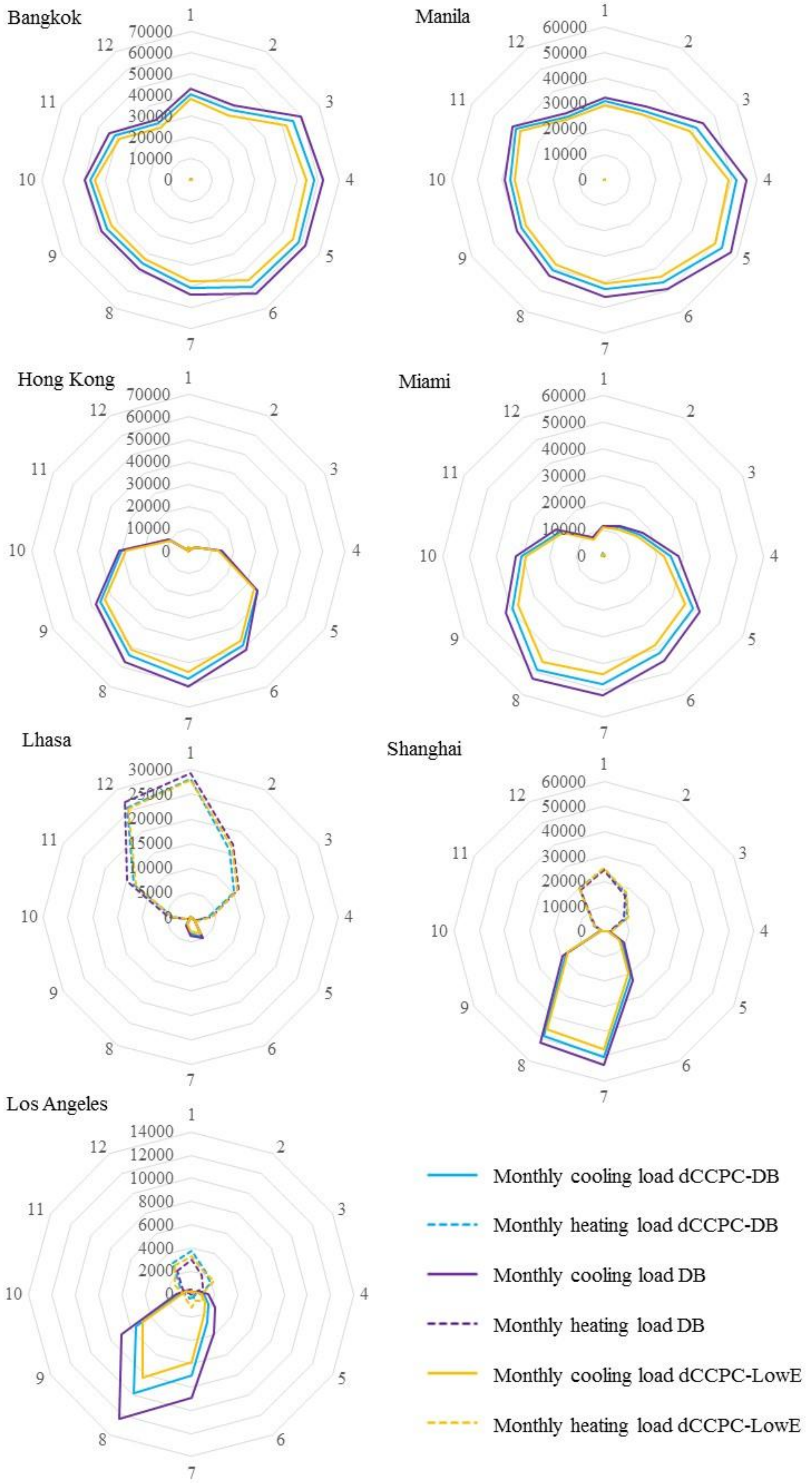

Bangkok
Manila
Hong Kong
Miami
Lhasa
Shanghai
Los Angeles
Monthly cooling load dCCPC-DB
Monthly heating load dCCPC-DB
Monthly cooling load DB
Monthly heating load DB
Monthly cooling load dCCPC-LowE
Monthly heating load dCCPC-LowE

Figure 9(b)

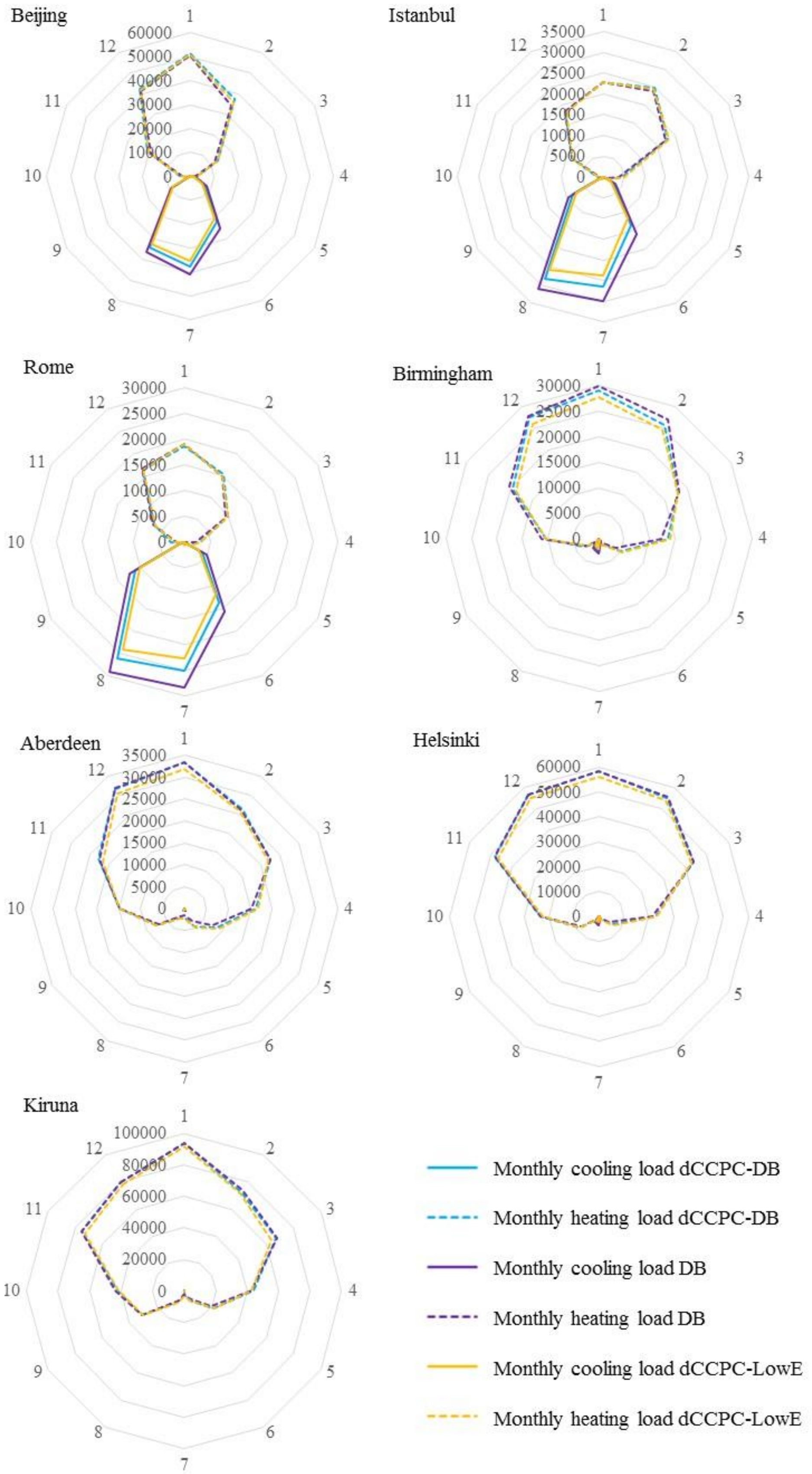
Beijing
Istanbul
Rome
Birmingham
Aberdeen
Helsinki
Kiruna
Monthly cooling load dCCPC-DB
Monthly heating load dCCPC-DB
Monthly cooling load DB
Monthly heating load DB
Monthly cooling load dCCPC-LowE
Monthly heating load dCCPC-LowE

Figure 10

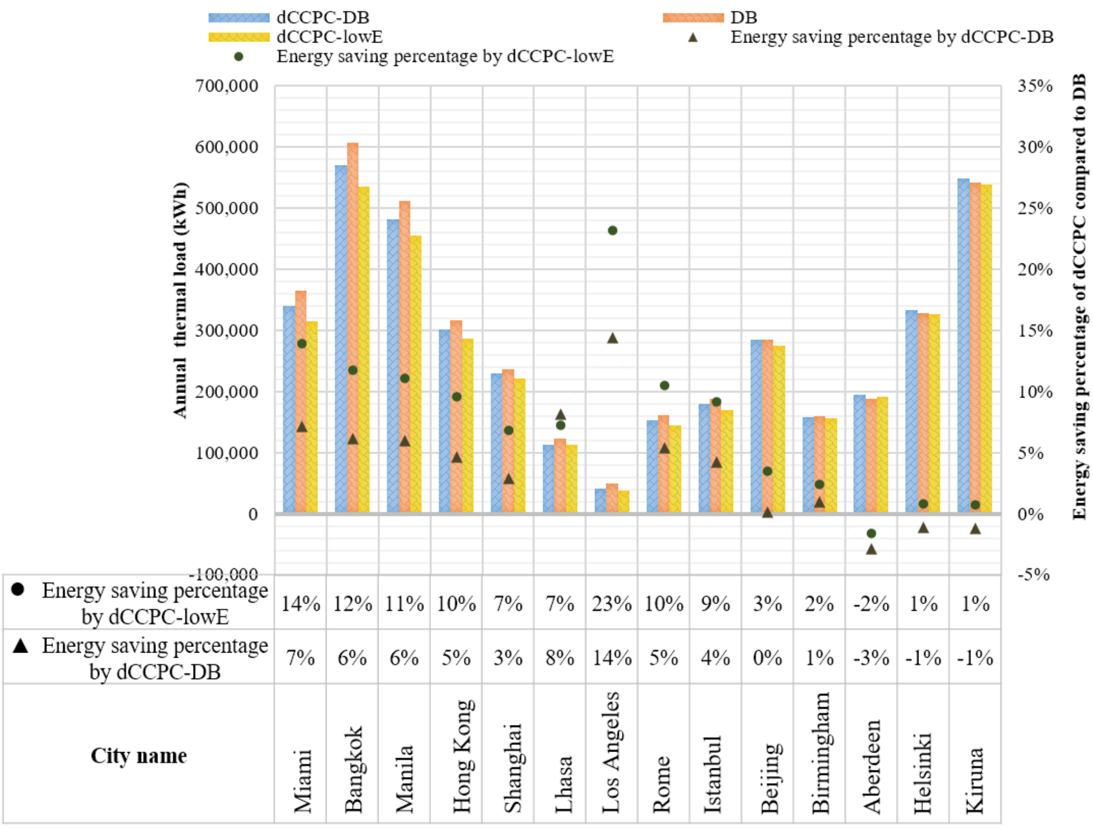

Figure 11

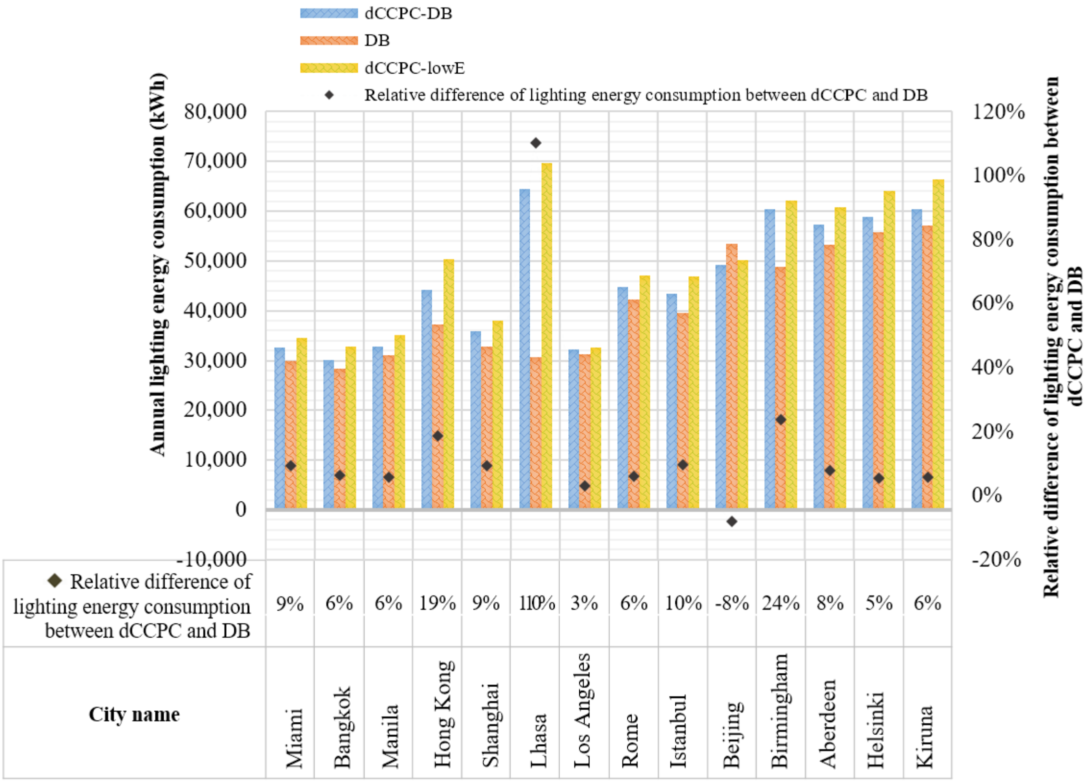

Figure 12

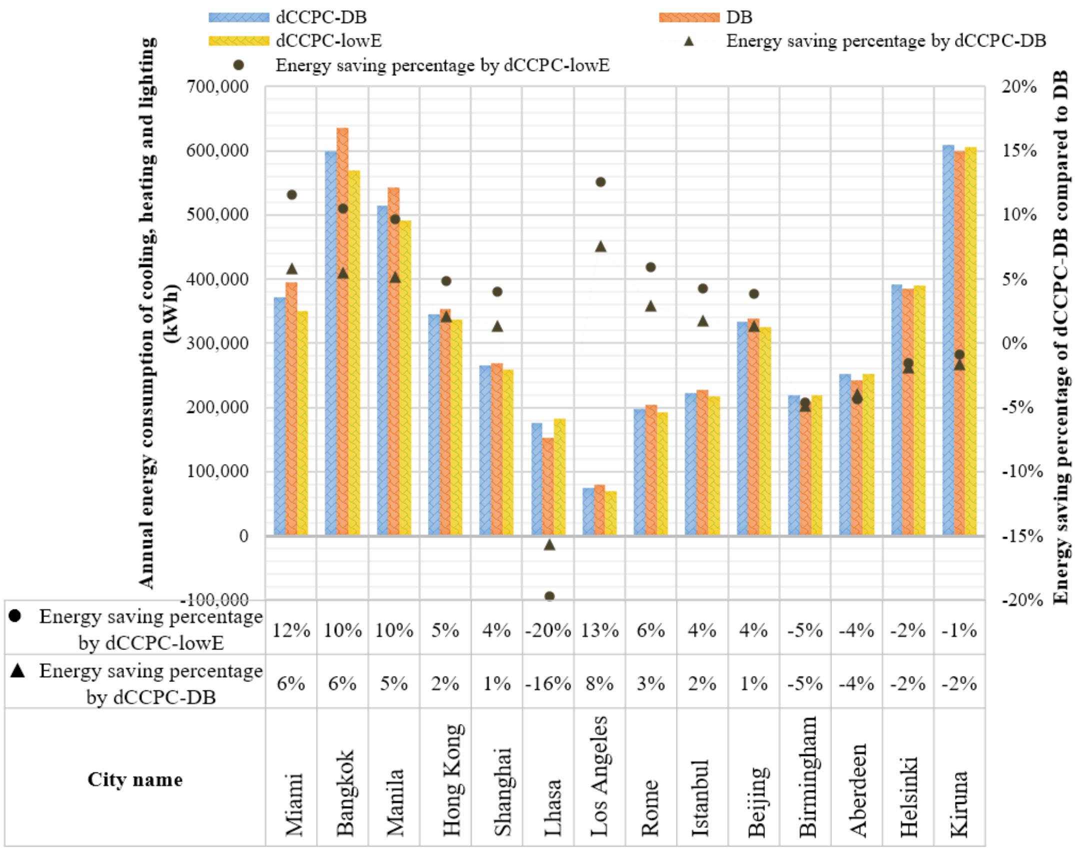

dCCPC-DB
DB
dCCPC-lowE
Energy saving percentage by dCCPC-DB
Energy saving percentage by dCCPC-lowE
Annual energy consumption of cooling, heating and lighting (kWh)
Energy saving percentage of dCCPC-DB compared to DB
700,000
600,000
500,000
400,000
300,000
200,000
100,000
0
-100,000
20%
15%
10%
5%
0%
-5%
-10%
-15%
-20%
Energy saving percentage by dCCPC-lowE: 12% 10% 10% 5% 4% -20% 13% 6% 4% 4% -5% -4% -2% -1%
Energy saving percentage by dCCPC-DB: 6% 6% 5% 2% 1% -16% 8% 3% 2% 1% -5% -4% -2% -2%
City name
Miami
Bangkok
Manila
Hong Kong
Shanghai
Lhasa
Los Angeles
Rome
Istanbul
Beijing
Birmingham
Aberdeen
Helsinki
Kiruna

Tables

Table 1

	Clear double glazing (DB)	Clear double glazing with dCCPC (dCCPC-DB)	Low-E double glazing with dCCPC (dCCPC-lowE)
U-value (W/m^2K)	2.669	2.669	1.420
SHGC	0.70	$T_{dCCPC} \times 0.70$	$T_{dCCPC} \times 0.27$
VT	0.79	$T_{dCCPC} \times 0.79$	$T_{dCCPC} \times 0.69$
T_{dCCPC}: Transmittance of dCCPC			

Table 2

Location		Latitude	Longitude	Köppen-Geiger climate classification	
Asia	China-Beijing	39.80°	116.47°	Dwa	Continental dry winter and hot summer climate
	China-Hong Kong	22.32°	114.17°	Cfa	Hot summer temperate without dry season climate
	China-Shanghai	31.17°	121.43°	Cfa	Hot summer temperate without dry season climate
	China-Lhasa	29.67°	91.13°	BSK	Arid steppe cold climate
	Philippines-Manila	14.52°	121.00°	Aw	Tropical savanna wet climate
	Thailand-Bangkok	13.92°	100.60°	Aw	Tropical savanna wet climate
Europe	Finland-Helsinki	60.32°	24.97°	Dfb	Warm summer continental without dry season climate
	UK-Aberdeen	57.20°	-2.22°	BSK	Arid steppe cold climate
	UK-Birmingham	52.45°	-1.73°	Cfb	Warm summer temperate without dry season climate
	Italy-Rome	41.80°	12.58°	Csa	Temperate dry and hot summer climate
	Sweden-Kiruna	67.82°	20.33°	Dfc	Hot summer continental without dry season climate
	Turkey-Istanbul	40.97°	28.82°	Csa	Temperate dry and hot summer climate
America	USA-Los Angeles	33.93°	-118.40°	Csa	Temperate dry and hot summer climate
	USA-Miami	25.80°	-80.27°	Aw	Tropical savanna wet climate

Table 3

Term	Calculation formula	Value of example	Step No.
β	$90^{\circ} - Latitude$	37.55°	1
$\Delta\gamma'$	Eq. (4)-(16)	22.86°	2
θ_h'	Eq. (17)	48.48°	3
Z'	$90^{\circ} - \theta_h'$	41.52°	4
I'	$I\cos\theta_i$	$220.13\,\mathrm{W/m^2}$	4
$I_h{}'$	$I_{total} - I'$	$52.87\,\mathrm{W/m^2}$	4
ε'	Eq. (18)	3.98	5
T_{dCCPC} from calculation	Eq. (2)	0.72	6
T_{dCCPC} from simulation	N/A	0.75	N/A

Table 4

Local time	Sky condition	dCCPC-double glazing (dCCPC-DB)			dCCPC-lowE		
		Experiment results	Simulation results	Errors	Experiment results	Simulation results	Errors
9:10	overcast	0.51	0.51	1.6%	0.45	0.44	1.2%
9:20	intermediate	0.63	0.57	10.8%	0.55	0.50	10.4%
9:30	overcast	0.58	0.55	6.7%	0.51	0.48	6.3%
9:40	overcast	0.54	0.51	5.3%	0.47	0.45	4.9%
9:50	clear	0.56	0.57	2.4%	0.48	0.50	2.8%
10:00	clear	0.55	0.52	4.7%	0.48	0.46	4.3%
10:10	clear	0.53	0.51	3.0%	0.46	0.45	2.6%
10:20	clear	0.50	0.51	2.8%	0.43	0.45	3.2%
10:30	intermediate	0.47	0.51	7.1%	0.41	0.44	7.5%
10:40	intermediate	0.42	0.47	9.6%	0.37	0.41	10.0%
10:50	clear	0.46	0.40	16.1%	0.40	0.35	15.6%
11:00	clear	0.36	0.37	1.8%	0.32	0.32	2.1%
11:10	clear	0.39	0.40	4.1%	0.34	0.35	4.4%
11:20	clear	0.31	0.33	5.7%	0.27	0.29	6.0%
11:30	overcast	0.45	0.50	9.1%	0.39	0.43	9.5%
11:40	overcast	0.45	0.49	7.9%	0.39	0.43	8.2%
11:50	intermediate	0.47	0.46	1.6%	0.41	0.40	1.2%
12:00	clear	0.38	0.35	10.0%	0.33	0.30	9.6%
RMSE		3.33%			2.89%		